# Evolution of Parinacota volcano, Central Andes, Northern Chile

**Jorge E. Clavero**
Servicio Nacional de Geología y Minería, Avda. Santa María 0104, Santiago, Chile
jclavero@sernageomin.cl
Department of Earth Sciences, University of Bristol, Wills Memorial Building, Queen's Road, BS8 1RJ, Bristol, U.K.

**R. Stephen J. Sparks**
Department of Earth Sciences-University of Bristol, Wills Memorial Building, Queen's Road,BS8 1RJ, Bristol, U.K
steve.sparks@bris.ac.uk

**Edmundo Polanco**
Servicio Nacional de Geología y Minería, Avda. Santa María 0104, Santiago, Chile
epolanco@sernageomin.cl

**Malcolm S. Pringle**
Scottish Universities Reactor and Research Center (SURRC), East Kilbride G75 0QF, UK
mpringle@surrc.ac.uk

## ABSTRACT

Parinacota is an active composite stratovolcano located in the Central Andes of Northern Chile (18°S). During its earlier stage (Parinacota 1 unit, Late Pleistocene, 300-70? ka) rhyolitic to andesitic magmas were erupted, forming a voluminous lava-dome complex with its associated pyroclastic fans (mainly block-and-ash flow deposits), essentially deposited towards the Upper Lauca basin (West). It later evolved to a steep-sided composite stratocone (Parinacota 2 unit, Late Pleistocene-Holocene, 70?-8 ka), mainly formed by andesitic lava flows and scoria tephra fallout deposits. Around 8 ka ago the ancestral Parinacota volcano, built during Parinacota 1 and 2, partially collapsed towards the west, in a single and catastrophic event generating the outstanding Parinacota Debris Avalanche deposit. Soon after the collapse a new stratocone started to build with the emission of andesitic lava flows and pyroclastic flows, and their associated fallout deposits (Parinacota 3 unit, Holocene, <8 ka). Some lahars mainly directed towards the south, west and east have also been generated during Parinacota 3. Contemporaneously with the formation of the central cone, a series of flank cones and their associated basaltic andesite to andesitic lava flows were formed (Ajata centres, 6-1.4 ka). These centres erupted through two fractures, NNE and NS oriented, in the south-western flank of the volcano. The new cone (Parinacota 3 unit) has an estimated minimum volume of 18 $km^3$, giving a minimum eruption rate of 2.25 $km^3\ ka^{-1}$ for the last 8,000 years, which means that Parinacota volcano must be considered one of the most active volcanoes in the Central Andes of Northern Chile during the Holocene.

*Key words: Eruption rate, Debris avalanche, Holocene, Parinacota, Chile.*

## RESUMEN

**La evolución del volcán Parinacota, Andes Centrales, norte de Chile.** El volcán Parinacota es un estratovolcán activo ubicado en los Andes Centrales del norte de Chile (18°S). Durante su primera etapa de evolución (Unidad Parinacota 1, Pleistoceno Superior, 300-70? ka) emitió magmas de composición riolítica a andesítica, formando un voluminoso complejo de lavas-domo con abanicos piroclásticos asociados (esencialmente depósitos de bloques y

ceniza), distribuidos principalmente hacia la parte superior de la cuenca del río Lauca (oeste). Posteriormente, evolucionó a un estratocono compuesto, de fuertes pendientes (Unidad Parinacota 2, Pleistoceno-Holoceno, 70?-8 ka), formado principalmente por lavas y depósitos de caída andesíticos. Aproximadamente hace 8 ka el volcán Parinacota ancestral, construido durante las unidades Parinacota 1 y 2, colapsó parcialmente hacia el oeste, en un evento único y catastrófico generando el Depósito de Avalancha de Parinacota. Poco tiempo después del colapso comenzó a edificarse un nuevo estratocono a través de la emisión de lavas y flujos piroclásticos andesíticos, con depósitos de caída asociados (Unidad Parinacota 3, Holoceno, <8 ka). Lahares dirigidos esencialmente hacia el sur, oeste y este también han sido generados en el Holoceno. Contemporáneamente con la edificación del nuevo cono, se formó una serie de conos de piroclastos de flanco y lavas andesítico-basálticas asociadas (volcanes de Ajata, 6-1,4 ka). Estos centros aprovecharon fracturas de orientación NNE y NS ubicadas en el flanco suroeste del volcán. El nuevo cono (Unidad Parinacota 3) tiene un volumen estimado de 18 $km^3$, lo que resulta en una tasa eruptiva de 2,5 $km^3\ ka^{-1}$ en los últimos 8.000 años. Esto significa que el volcán Parinacota debe ser considerado uno de los más activos de los Andes Centrales del Norte de Chile en el Holoceno.

*Palabras claves: Tasa de erupción, Avalancha de escombros, Holoceno, Parinacota, Chile.*

## INTRODUCTION

Parinacota volcano is located in the Central Andes Volcanic Zone, in the border between Chile and Bolivia (18°10'S, Fig. 1) and, together with Pomerape volcano (Figs. 1, 2), forms the Nevados de Payachata volcanic area. Parinacota (Flamingo Lake in Aymara's language) is a composite volcano of Late Quaternary age with an almost perfect conic-shaped edifice mainly formed by andesitic lava flows built on top of an andesitic-rhyolitic lava-dome complex, which itself was built on top of Pleistocene lacustrine deposits (Clavero, 2002; Stern, 2004). Its present summit (crater rim) reaches 6,350 m a.s.l., where a 500 m diameter and *ca.* 100 m deep crater is located. It has a permanent ice cap above 5,500 m, which covers an area of about 4 $km^2$. The volcano and its products, including the Parinacota debris avalanche deposit, have a minimum estimated volume of 45 $km^3$. Its location in a very high plateau, which is affected by tropical easterly precipitation, provides a context for understanding its Late Pleistocene-Holocene evolution in terms of palaeoclimatic changes. In recent times this area receives an annual precipitation of about 440 mm with 90% occurrence from November to March, and has a mean annual temperature of 1°C with diurnal fluctuations of as much as 30°C (Schwalb *et al.*, 1999 and references therein).

Here the authors describe the evolution of Parinacota volcano and its relationship with its surrounding environment, based on new mapping (1:25,000 scale) carried out in the Altiplano of northern Chile, as part of the Chilean Geological Survey (Servicio Nacional de Geología y Minería) mapping program, as well as new geochronological ($^{40}Ar/^{39}Ar$ and radiocarbon) and geochemical data, and indications of recent activity from Aymara people legends.

## PREVIOUS WORK

The first geologic reconnaissance map (1:50,000 scale) of the Nevados de Payachata volcanic area was done by Katsui and González (1968). Together with petrographic data they suggested a five-stage eruptive history for Parinacota volcano. They interpreted the edifice as entirely Holocene despite the lack of gechronologic data. Francis and Self (1987) and Francis and Wells (1988) reinterpreted the widespread deposits located to the west of Parinacota volcano as being debris avalanche deposits produced by a sector collapse, mainly based on satellite data. There have also been several detailed petrological and geochemical investigations on the Nevados de Payachata volcanic area (Wörner *et al.*, 1988; Davidson *et al.*, 1990; Wörner *et al.*, 1992a; Wörner *et al.*, 1992b;

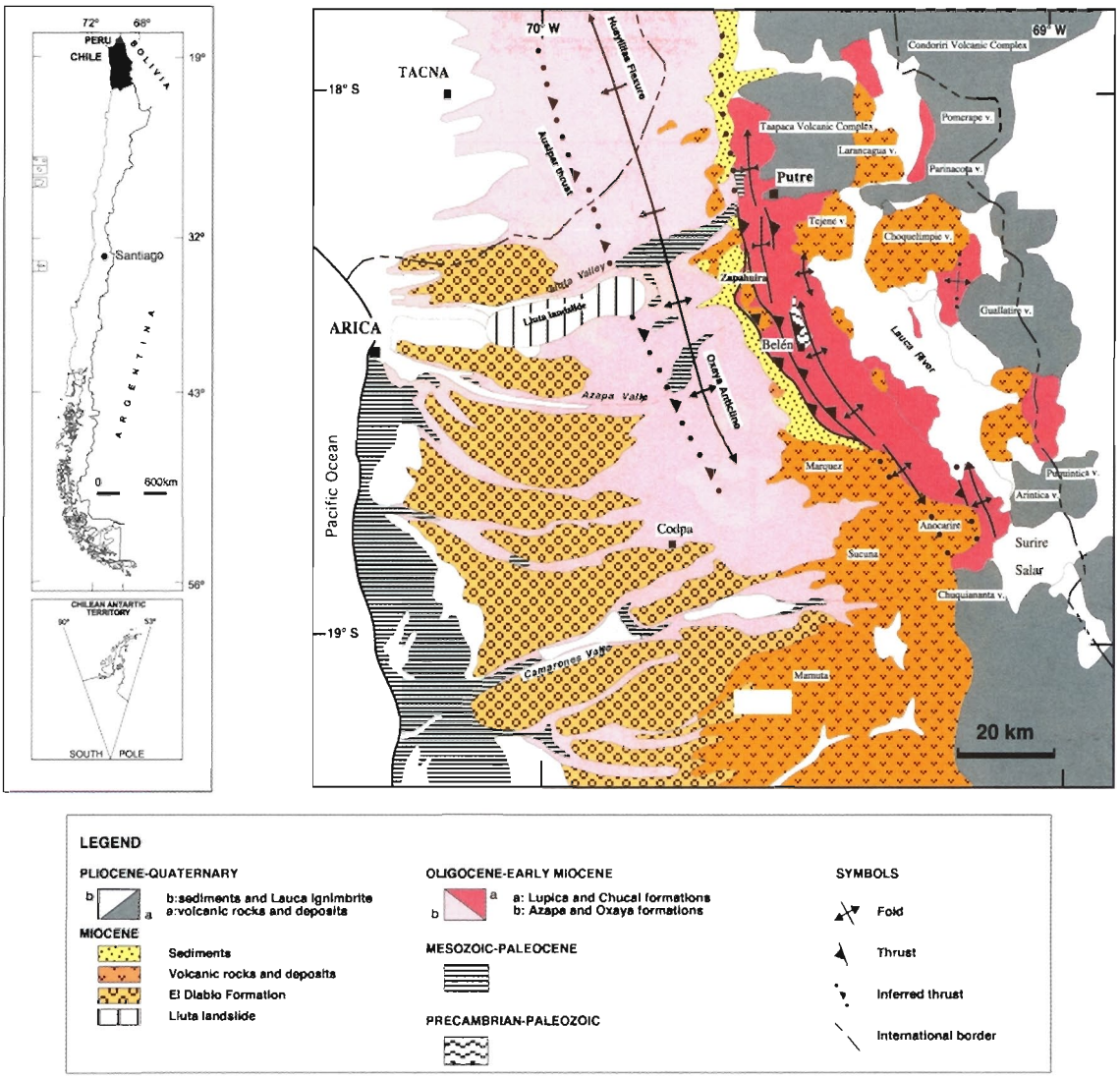


FIG. 1. Location map of the study area and regional geologic map of Northern Chile (modified from García, 2001).

Entenmann, 1994; Bourdon *et al.*, 2000; Wörner *et al.*, 2000a). Wörner *et al.* (1988) reinterpreted the evolution of Parinacota volcano given by Katsui and González (1968), retaining the five evolutionary stages. Clavero *et al.* (2002) presented a detailed study of the Parinacota debris avalanche deposit and its possible origin, transport and emplacement mechanisms.

## GEOLOGIC SETTING

Parinacota volcano is built on the high Andean plateau known as the Altiplano (Fig. 1), which is confined between two main mountain chains elongated in a north-south direction, the Cordillera Oriental and Cordillera Occidental (eastern and western cordilleras) and has an average altitude of

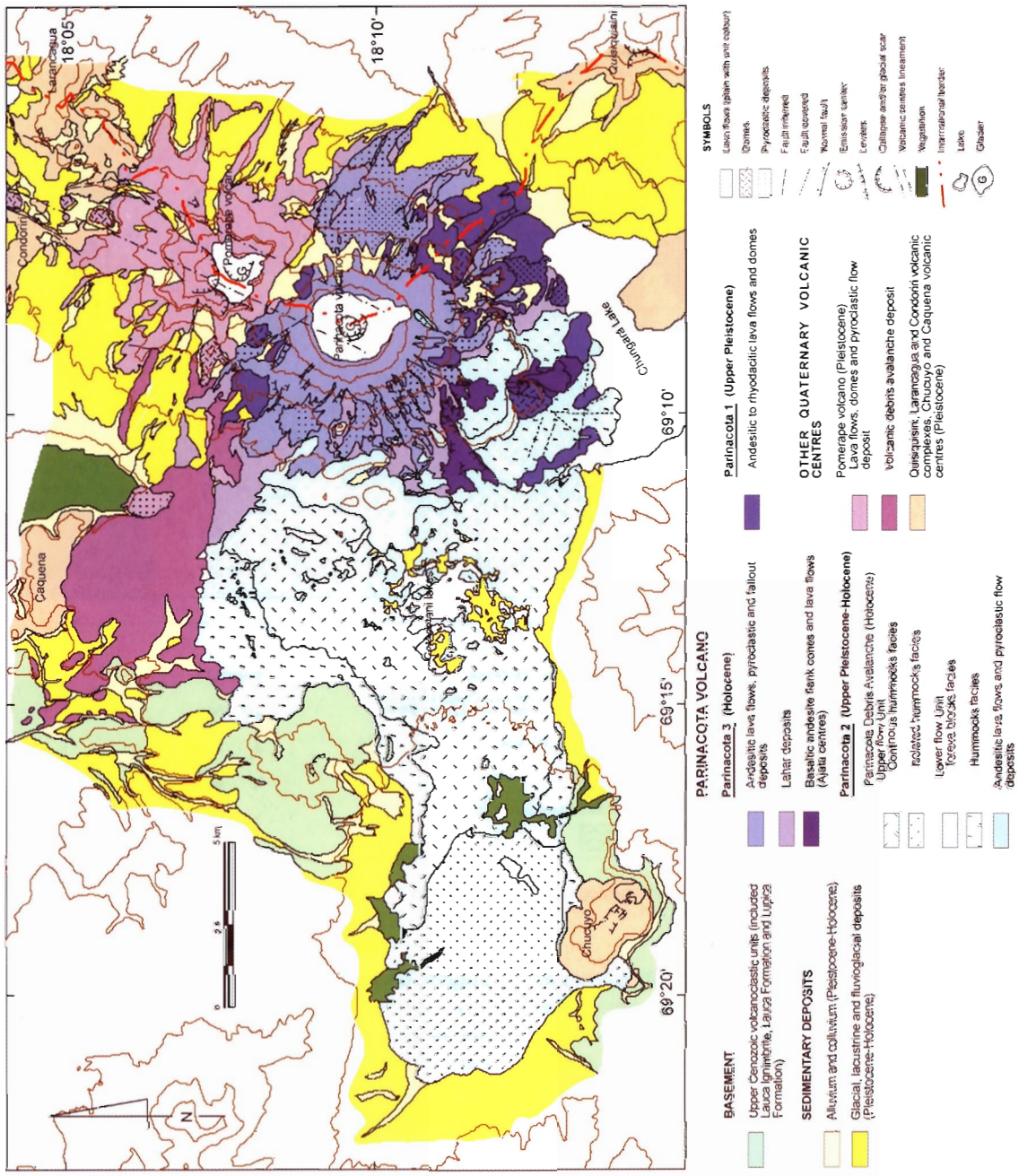


FIG. 2. Geologic map of Parinacota volcano and surrounding areas (modified from 1:40,000 scale map of Clavero, 2002).

4,000 m a.s.l. Rocks of the western cordillera range in age from pre-Cambrian to Miocene (Pacci *et al.*, 1980; Wörner *et al.*, 2000b; García, 2001; García *et al.*, 2004; Pinto *et al.*, 2004; Fig. 1), which were uplifted on a west-vergent thrust system mainly during the Miocene (Muñoz and Sepúlveda, 1992; Muñoz and Charrier, 1996; García *et al.*, 1999; García, 2001). The crustal thickness exceeds here 70 km (Allmendinger *et al.*, 1997; Scheuber and Giese, 1999).

### BASEMENT OF QUATERNARY VOLCANOES

In the Nevados de Payachata area, the oldest basement units are located in the western part (Fig. 2) and are mainly formed by Oligocene to Miocene volcaniclastic sequences and younger Miocene-Pleistocene sedimentary and volcanic deposits. The volcaniclastic sequence (the Lupica Formation of Upper Oligocene-Lower Miocene age; Montecinos, 1963; García, 2001; García *et al.*, 2004) is mainly formed by rhyolitic welded ignimbrites and epiclastic sandstones (dipping 30°west). In the south-western part of the area, near the Chucuyo volcanic centre (Fig. 2), distal laharic breccias and lava flows from the Upper Miocene Ajoya volcano crop out (Aguirre, 1990; García *et al.*, 2004). During the Miocene (?) to Pliocene an intravolcanic basin formed and was partially filled by lacustrine sediments and epiclastic deposits (Lauca Formation, Kött *et al.*, 1995; Gaupp *et al.*, 1999), which were partly buried by the Lauca Ignimbrite of Upper Pliocene age (2.7 Ma; Kött *et al.*, 1995; Wörner *et al.*, 2000a; García *et al.*, 2004). The northeastern area of this basin, which is now partly buried by Parinacota volcano and its debris avalanche deposits (Fig. 2), was later reactivated as a lacustrine basin during the Pleistocene (Clavero *et al.*, 2002; García *et al.*, 2004).

### OTHER TERTIARY VOLCANIC CENTRES

As part of the main Central Andes Volcanic Zone, Parinacota volcano is located among several Quaternary volcanic centres (Figs. 1, 2), which are mostly located along the border of Bolivia and Chile, the closest to Parinacota volcano are briefly described here. Among the most important ones are: Condoriri Volcanic Complex (Ar-Ar age of 0.650± 0.070 Ma); Larancagua Volcanic Complex (no radiometric dates available); Quisiquisini volcano (K-Ar age of a lava 1.0±0.1 Ma); Chucuyo and Caquena volcanic centres (K-Ar ages of 275±44 ka and 285±53 ka, respectively) and finally Pomerape volcano. This last one consists of a stratocone mainly formed by andesitic to dacitic lava flows, domes and pyroclastic flow deposits, partially affected by deep glacial erosion and, at least, one sector collapse directed towards the west, which generated a voluminous debris avalanche deposit (K-Ar dates of 106±7 ka and 205±24 ka). Age data are from Wörner *et al.* (1988; 2000a) and García *et al.* (2004). A new $^{40}Ar/^{39}Ar$ (305.8±3.2 ka, Table 1) date is presented here for a rhyodacitic pyroclastic flow deposit.

## ANALYTICAL TECHNIQUES

### $^{40}Ar/^{39}Ar$

Six samples were selected (five from Parinacota and one from Pomerape volcano) following the petrographic criteria of Maniken and Dalrymple (1972), mainly choosing holocrystalline (as much as possible) unaltered rocks, representative of the major stratigraphic units of Parinacota volcano. Where pyroclastic deposits were selected, the authors used standard criteria to select primary hot blocks, such as PJB (Prismatically Jointed Blocks, *i.e.*, Cas and Wright, 1987).

Mineral and groundmass separates were loaded in 99.99% copper foil packets. Neutron flux standards were loaded in aluminium foil packets, and loaded in 6 mm (internal diameter) quartz vials at intervals between 20 to 30 mm, intercalated with the samples. The monitor mineral used was the 27.92 Ma USGS sanidine 85G003 from the Taylor Creek rhyolite (Dalrymple and Duffield 1988). The quartz vials were irradiated at 1 MW for 30 minutes in the Cd-shielded CLICIT facility at the Oregon State University Triga reactor, USA.

After two to twelve months the samples were

**TABLE 1. $^{40}Ar/^{39}Ar$ GEOCHRONOLOGY DATA AND AGES OF NEVADOS DE PAYACHATA VOLCANOES.**

| Sample | UTM Coordinates N | E | Unit/rock | Material | Whole-rock $K_2O$ (wt%) | Total K/Ca | Total Arad mol/g | Total fusion age (ka) ± 1s | N | Increments used (°C) | $^{39}Ar$ (%) Age ±1σ (ka) | Age spectrum analysis MSWD | SUMS | Inverse isochron analysis $^{40}Ar/^{36}Ar$±1σ intercept | Age±1σ ka |
|---|---|---|---|---|---|---|---|---|---|---|---|---|---|---|---|
| Parinacota volcano | | | | | | | | | | | | | | | |
| CAL-7 | 7985228 | 479663 | 2/Cryptodome | Groundmass | 3,43 | 1,569 | 4,14E-14 | 0.15±4.5 | 6 of 12 | 567-907 | 55,8 | 7.1 ± 3.3 | 2,03 | 2,82 | 294.0±4.0 | 13.9±20.5 |
| CAL-10 | 7990765 | 481490 | 1/Block-and-ash | Biotite | 4,25 | 55,720 | 5,11E-14 | 275.6±11.0 | 10 of 32 | 784-968 | 53,4 | 76.2±8.2 | 5,77 | 4,97 | 294.9±0.8 | 77.9±12 |
| CAL-51 | 7987500 | 481450 | 1/Block-and-ash | Biotite | 4,45 | 13,641 | 5,89E-14 | 338.4±13 | 9 of 25 | 1023-1077 | 66,9 | 302.9±7.1 | 3,14 | 4,43 | 296.5±2.0 | 289.6±27 |
| CAL-51 | 7987500 | 481450 | 1/Block-and-ash | Hornblende | 4,45 | 0,593 | 1,19E-14 | 362.2±25 | 5 of 13 | 1011-1180 | 73,2 | 308.0±12.0 | 1,44 | 2,27 | 295.5±1.5 | 307.7±25 |
| CAL-88 | 7989250 | 482500 | 2/lava (av. scar) | Groundmass | n-a | 0,776 | 3,80E-14 | 24.9±4.7 | 9 of 16 | 633-1011 | 46,7 | 14.1±3.2 | 1,07 | 1,76 | 296,1±2.1 | 10.5±10.3 |
| CAL-91 | 7986300 | 481750 | 1/Dome | Biotite | n-a | 76,774 | 4,22E-14 | 169.1±13.0 | 7 of 17 | 907-1053 | 73 | 138.9±21.4* | 13.64* | 8.47* | 301.1±2.9 * | 62.4±46.2 |
| Pomerape volcano | | | | | | | | | | | | | | | | |
| CAL-20 | 7998150 | 479301 | Pyr. Flow | Biotite | 4,10 | 13,209 | 4,96E-14 | 282.8±14.8 | 14 of 19 | 816-1122 | 92,6 | 305.8±3.2 | 2,99 | 4,55 | 295.1±1.0 | 309.2±7.3 |

n-a: not available.

N: number of heating increments used in regression.

*: not reliable age (see text for discussion).

In bold: the prefered age for each sample.

analyzed at SURRC (Scottish Universities Research and Reactor Centre, UK). Incremental step-heating experiments comprising twelve to thirty two steps were carried out in a double vacuum resistance furnace, attached to a small volume gas clean-up system with SAES Zr-Al C50 getters at 400° C and a zeolite finger. Temperatures reported for incremental steps are as calibrated by optical pyrometry. After 15 minutes heating and 10 to 15 minutes further cleanup with an additional Zr-Al C50 getter at room temperature, isotopic analysis of the purified gas was carried out on an ultrasensitive rare-gas mass spectrometer (Mass Analyser Products 215), with a modified Nier source and variable slit. The mass discrimination was carefully monitored, due to its particular significance for young samples which contain large amounts of atmospheric argon compared to small amounts of radiogenic argon, by regularly analyzing aliquots of air ($^{40}Ar/^{36}Ar = 295.5$) from an on-line gas bulb and pipette system.

Based on previous work (Wijbrans *et al.*, 1995), the reactor corrections for interfering neutron-induced reactions of $^{40}K$ and $^{40}Ca$, are as follows:

$$[^{40}Ar/^{39}Ar]_K = 0{,}00086;\ [^{36}Ar/^{37}Ar]_{Ca} = 0{,}000264;$$
$$[^{39}Ar/^{37}Ar]_{Ca} = 0{,}000673$$

The decay constants of Steiger and Jäger (1977) were used in age calculations. J values were determined from the mean of five laser fusion analyses from each monitor packet. Comparison of the J curve to individual monitor estimates suggest a conservative error in J for samples is 0.3-0.5%.

Sample ages were calculated from both plateau and isochron analysis. Plateau ages were calculated as weighted means, where each age is weighted by the inverse of its variance (Taylor, 1982) and involve a single variable MSWD calculation to test for excess scatter. Isochron ages were calculated using the cubic least squares regression with correlated errors (York, 1969). All errors are reported as one standard deviation of the analytical precision, and all significant tests are done at the 95 % confidence level.

Full discussion of results, as well as more detailed petrographic descriptions of the units, can be found *in* Clavero (2002).

## RADIOCARBON

Samples of peat, paleosoil, organic-rich fallout ash layers and carbonised grass contained in pyroclastic flow deposits were taken in the field, avoiding contamination with young carbon, and packed in aluminium foil packets. Conventional analyses were carried out at Isotrace Radiocarbon Laboratory (University of Toronto, Canada) and AMS analyses were performed at Rafter laboratories (New Zealand).

Sample ages are quoted as uncalibrated conventional radiocarbon dates in years before present (BP, with present=1950 AD), using the Libby $C^{14}$ mean life of 8033a. The errors represent the 68.3% limit.

## GEOCHEMISTRY

Twenty samples were selected in the field in order to be representative of all three evolutionary stages of Parinacota volcano. Unaltered rocks were taken (half to 1 kg), avoiding slightly to strongly hydrothermally altered rocks.

Major and trace element chemical analyses were carried out at the Servicio Nacional de Geología y Minería (SERNAGEOMIN, CHILE). Samples were crushed under 200 sieve and then analysed with an AAS (Atomic Absorption Spectrometry) for major oxides, and with an ICP-AES (Inductive Coupled Plasma-Atomic Emission Spectrometry) for trace elements. Errors in the methods used by SERNAGEOMIN geochemical laboratory are usually less than 0.5% for major oxides. These results are permanently calibrated with international standards.

**TABLE 2. STRATIGRAPHIC DIVISIONS OF PARINACOTA VOLCANO ACCORDING TO KATSUI AND GONZÁLEZ (1968); WÖRNER *et al.* (1988) AND THIS STUDY.**

| Katsui and González (1968) | | | Wörner *et al.* (1988) | | | This study | | |
|---|---|---|---|---|---|---|---|---|
| **Stage** | **Definition** | **Age** | **Stage** | **Definition** | **Age** | **Stratigraphic unit** | **Definition** | **Age** |
| I | Andesitic lava flows (at the base of the edifice). | Holocene | I | Ia: Andesitic lava flows<br>Ib: Rhyolitic domes and associated block-and-ash flows. | Late Pleistocene (110-264 ka) | 1 | Rhyolitic to rhyodacitic domes and their associated block-and-ash flow deposits;andesitic and dacitic lavas and dacitic lava coulées. | Late Pleistocene (300-70? ka) |
| II | Rhyolitic domes. | Holocene | II | Old cone, formed by rhyodacitic flows and domes. | Late Pleistocene (12-53 ka) | 2 | Ancestral Parinacota stratocone, mainly formed by andesitic lava flows (amphibole-rich and two-pyroxene) and pyroclastic fallout deposits. End of unit with the collapse of the edifice at 8 ka generating the Parinacota debris avalanche deposit. | Late Pleistocene-Holocene (70?-8 ka) |
| III | Andesitic lava flows of the main cone. | Holocene | III | Debris avalanche with dacite bombs and plinian pumice. | Late Pleistocene (13.5 ka) | 3 | New cone, mainly formed by andesitic lava flows, pyroclastic flow and fallout deposits and lahar deposits. Simultaneously (6-1.4 ka) formation of the flank Ajata centres (basaltic andesite to andesitic composition). Youngest eruptions originated from the central cone (forming pyroclastic flows and tephra fallout). | Holocene (<8ka) |
| IV | Andesitic lava flows and pyroclastic fallout deposits more basic than Stage III (including the Cotacotani lava field, later interpreted by others as a debris avalanche). | Holocene | IV | Second cone building stage (lava and pumice flows, no amphibole) | Late Pleistocene-Holocene | | | |
| V | Flank parasite cones and lavas from Ajata centres. Similar composition to main cone lavas. | Holocene | V | Sub-recent mafic satellite cinder cones and lava flows (Ajata centres). | Recent | | | |

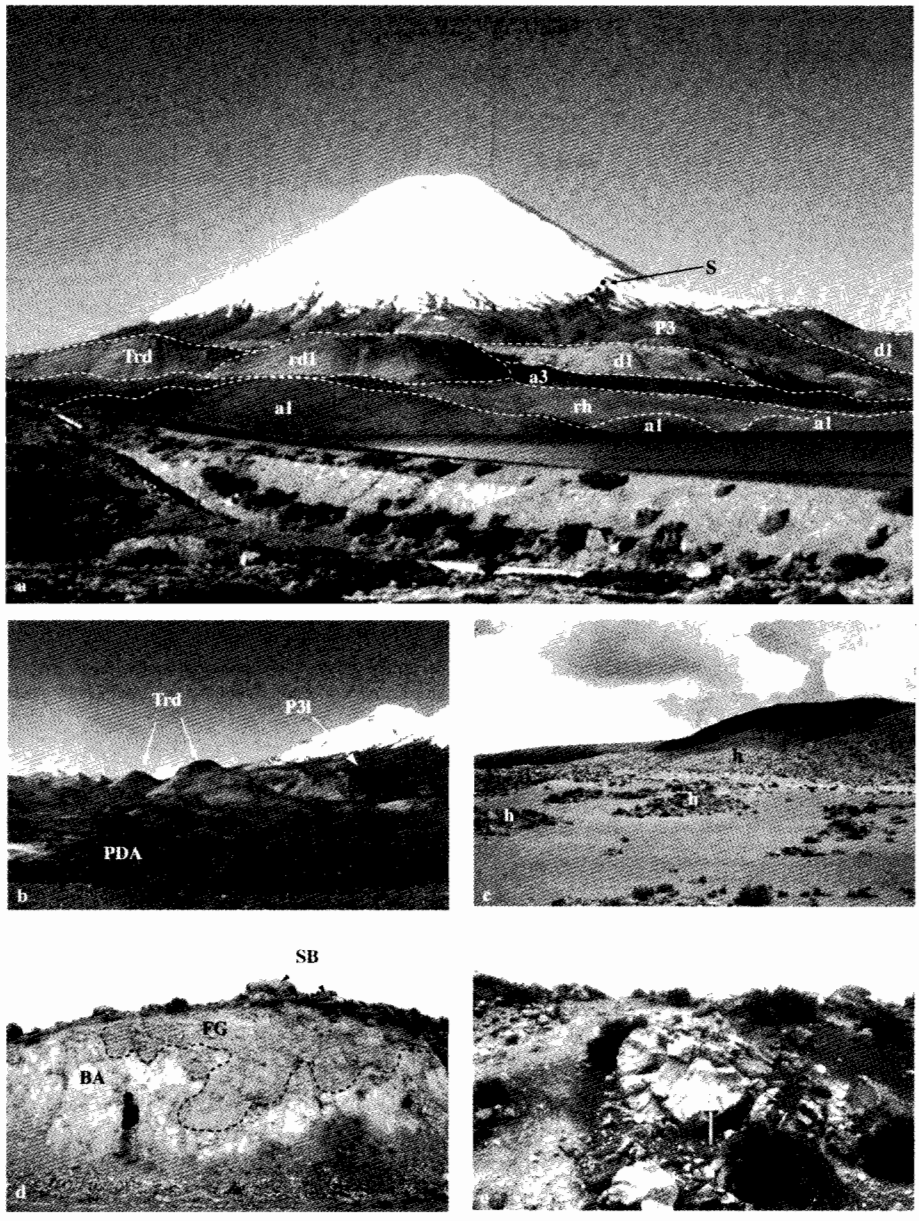


FIG. 3. **a.** Parinacota volcano viewed from the south. The remnant of the Parinacota Avalanche scar can be seen on its southern flank (marked S), as well as some of its units. rd1: Parinacota 1 rhyolitic domes, Trd: Parinacota Debris Avalanche Toreva blocks made of Parinacota 1 rhyolitic domes, rh: Parinacota Debris Avalanche hummocks made of Parinacota 1 rhyolitic block-and-ash flow deposits, d1: Parinacota 1 dacitic coulées, a1: Parinacota 1 andesitic lavas, a3: Parinacota 3 flank andesitic lava of the southern Ajata centres, P3: Parinacota 3 andesitic lavas forming the main post-collapse stratocone; **b-** proximal facies of the Parinacota Debris Avalanche viewed from the south-west, Pomerape volcano can be seen in the background. Trd symbol shows Toreva blocks of the avalanche formed by large tilted blocks of Parinacota 1 rhyolitic domes, P3l shows a Parinacota 3 andesitic lava flow overlying a Toreva block and PDA shows the Parinacota Debris Avalanche upper flow unit hummocks.; **c-** Parinacota Debris Avalanche lower unit hummocks (marked h) in the northern part of the study area, essentially made of Parinacota 1 rhyodacitic block-and-ash flow deposits; **d-** Parinacota Debris Avalanche lower unit hummock showing the incorporation of fluvioglacial deposits (FG) and Parinacota 1 rhyolitic block-and-ash flow deposits (BA) into the avalanche. Scattered blocks of the upper flow unit can be seen on top of the hummock (SB); **e-** Detail of a Parinacota Debris Avalanche lower flow unit hummock, showing remnants of PJB blocks from Parinacota 1 rhyodacitic block-and-ash flow deposits. Hammer is 30 cm long.

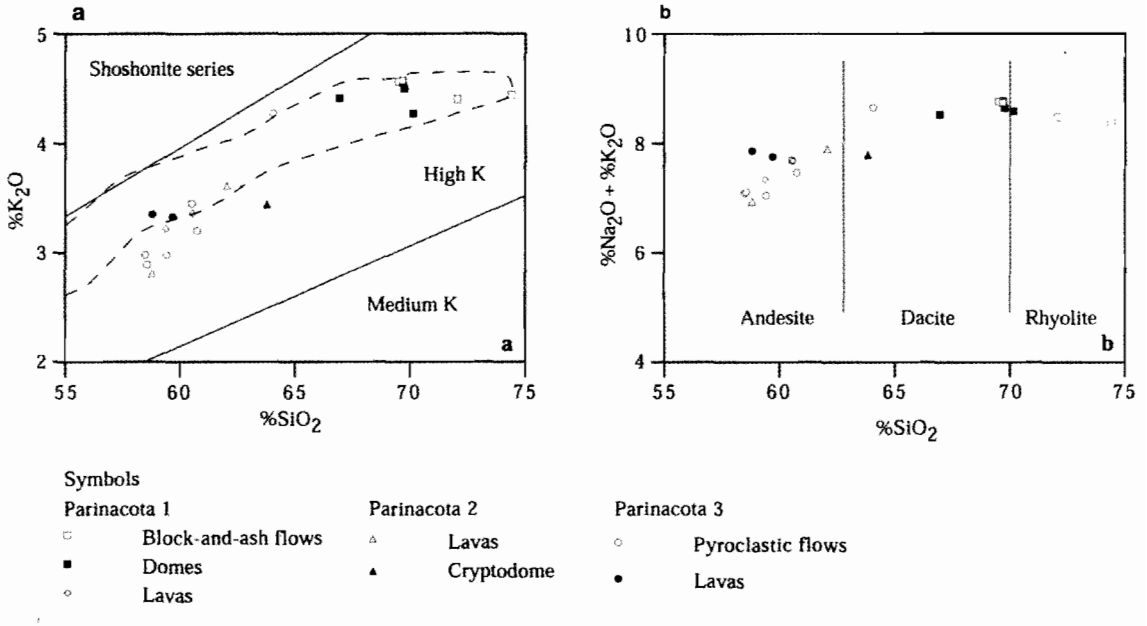


FIG. 4. **a-** $K_2O$ *versus* $SiO_2$ diagram of Parinacota volcano units. High and Medium-K fields taken from Le Maitre *et al.* (1989). Dashed line marks the area where samples from Wörner *et al.* (1988) and Davidson *et al.* (1990) fall; **b-** total alkali *versus* silica diagram with basic classification of Parinacota volcano units.

## GEOLOGY OF PARINACOTA VOLCANO

The authors divide the volcanic evolution of Parinacota volcano into three stratigraphic units. Table 2 summarizes this new scheme, compared to the previous suggested for Parinacota volcano.

### PARINACOTA 1 UNIT (LATE PLEISTOCENE, 300-70? KA)

This unit includes andesitic lavas, dacitic coulées and rhyodacitic to rhyolitic domes and block-and-ash flow deposits. Four whole-rock K-Ar dates presented by Wörner *et al.* (1988), range in age from 110±22 ka to 264±16 ka. Here are 2 more dates reported (Table 1) from rhyodacitic block-and-ash flow deposits of this stage (76.2 ± 8.2 ka and 308.0 ± 12.0 ka) that were incorporated in the lower flow unit of the Parinacota Debris Avalanche (Clavero *et al.*, 2002). Ongoing research in the area indicates that this unit could reach up to 30 ka (B. Singer, written communication, 2004).

#### ANDESITIC LAVA FLOWS

Parinacota 1 andesite lavas are located in the northern shore of Chungará Lake and at the northwestern foot of the volcano (Figs. 2, 3a). The andesites (59-61% $SiO_2$, Fig. 4, Table 3) are 30-50 m thick and have smooth surfaces affected by glacial and alluvial erosion, without primary structures preserved. These porphyritic rocks (up to 20 vol.% phenocrysts) consist of a plagioclase-clinopyroxene-orthopyroxene-amphibole phenocryst assemblage.

#### RHYOLITIC TO RHYODACITIC DOMES AND BLOCK-AND-ASH FLOW DEPOSITS

There is only one in situ outcrop of this unit, located on the southern flank of the volcano (Figs. 2, 3a). All the rest were incorporated into the Parinacota Debris Avalanche (end of Parinacota 2

**TABLE 3. MAJOR ELEMENT GEOCHEMICAL DATA FROM PARINACOTA VOLCANO.**

| Sample | UTM Coordinates N | E | Unit | Rock/deposit | $SiO_2$ | $Al_2O_3$ | $TiO_2$ | $Fe_2O_3$ | FeO | CaO | MgO | MnO | $Na_2O$ | $K_2O$ | $P_2O_5$ | $H_2O$ | C | S | Total |
|---|---|---|---|---|---|---|---|---|---|---|---|---|---|---|---|---|---|---|---|
| CAL-41 | 7992300 | 481650 | 3 | Pyroclastic flow | 60.46 | 15.96 | 1.11 | 3.18 | 2.81 | 5.48 | 2.65 | 0.09 | 4.24 | 3.18 | 0.36 | 0.21 | 0.05 | 0.02 | 99.82 |
| CAL-41B | 7992300 | 481650 | 3 | Pyroclastic flow | 58.25 | 16.21 | 1.31 | 3.21 | 3.65 | 5.93 | 3.36 | 0.09 | 4.20 | 2.88 | 0.40 | 0.26 | | 0.03 | 99.78 |
| CAL-44 | 7995500 | 484200 | 3 | Pyroclastic flow | 60.27 | 15.51 | 1.18 | 2.67 | 3.19 | 5.48 | 3.16 | 0.08 | 4.22 | 3.44 | 0.38 | 0.13 | | | 99.70 |
| CAL-57 | 7989800 | 481750 | 3 | Lava flow | 57.55 | 16.08 | 1.30 | 3.00 | 3.38 | 5.42 | 2.94 | 0.08 | 4.41 | 3.28 | 0.43 | 1.96 | | | 99.83 |
| CAL-59 | 7990300 | 482050 | 3 | Lava flow | 59.36 | 15.62 | 1.34 | 3.03 | 3.47 | 5.47 | 2.95 | 0.08 | 4.41 | 3.31 | 0.42 | 0.39 | | | 99.85 |
| CAL-86 | 7987350 | 485400 | 3 | Pyroclastic flow | 58.78 | 16.29 | 1.18 | 3.00 | 3.45 | 5.69 | 3.10 | 0.09 | 4.02 | 2.95 | 0.37 | 0.45 | | 0.14 | 99.53 |
| CAL-164A | 7984547 | 487815 | 3 | Fallout deposit | 62.66 | 17.16 | 0.71 | 1.74 | 2.13 | 3.44 | 1.19 | 0.06 | 4.28 | 4.18 | 0.26 | 2.05 | | 0.01 | 99.87 |
| CAL-164B | 7984547 | 487815 | 3 | Fallout deposit | 58.13 | 16.59 | 1.32 | 3.06 | 3.61 | 5.91 | 3.25 | 0.10 | 4.08 | 2.96 | 0.37 | 0.35 | 0.08 | 0.03 | 99.84 |
| CAL-4A | 7986252 | 471291 | 2 | Lava flow/PDA | 58.35 | 15.70 | 1.33 | 4.09 | 2.52 | 6.12 | 3.67 | 0.09 | 4.09 | 2.79 | 0.46 | 0.50 | 0.05 | 0.01 | 99.78 |
| CAL-7 | 7985228 | 479663 | 2 | Cryptodome PJB | 63.24 | 15.66 | 0.91 | 2.44 | 2.17 | 4.38 | 2.05 | 0.08 | 4.33 | 3.43 | 0.39 | 0.52 | 0.03 | 0.01 | 99.63 |
| CAL-134 | 7988419 | 473020 | 2 | Lava flow/PDA | 61.45 | 15.54 | 1.07 | 3.51 | 1.84 | 4.65 | 2.73 | 0.08 | 4.25 | 3.57 | 0.33 | 0.81 | | | 99.83 |
| CAL-4 | 7986252 | 471291 | 1 | Block-and-ash flow | 71.66 | 14.00 | 0.36 | 1.58 | 0.52 | 1.91 | 0.74 | 0.05 | 4.06 | 4.37 | 0.18 | 0.33 | 0.04 | 0.01 | 99.80 |
| CAL-9 | 7989387 | 480188 | 1 | Block-and-ash flow | 73.20 | 12.95 | 0.25 | 0.91 | 0.64 | 1.47 | 0.51 | 0.04 | 3.87 | 4.37 | 0.17 | 1.38 | | 0.01 | 99.75 |
| CAL-10 | 7990765 | 481490 | 1 | Dome | 69.85 | 14.33 | 0.45 | 1.88 | 0.69 | 2.57 | 0.99 | 0.05 | 4.29 | 4.25 | 0.23 | 0.15 | 0.05 | | 99.77 |
| CAL-42 | 7995450 | 482850 | 1 | Lava flow | 59.90 | 15.48 | 1.21 | 3.18 | 2.86 | 5.30 | 2.90 | 0.08 | 4.27 | 3.32 | 0.41 | 0.96 | | | 99.86 |
| CAL-49 | 7996400 | 477700 | 1 | Pyroclastic flow | 68.41 | 14.44 | 0.55 | 1.34 | 1.17 | 2.43 | 1.04 | 0.05 | 4.09 | 4.49 | 0.16 | 1.70 | | | 99.87 |
| CAL-51 | 7987500 | 481450 | 1 | Block-and-ash flow | 67.91 | 14.18 | 0.58 | 2.54 | 0.24 | 2.41 | 1.05 | 0.05 | 4.10 | 4.45 | 0.18 | 2.28 | | | 99.97 |
| CAL-55 | 7987150 | 482250 | 1 | Dome | 69.22 | 14.28 | 0.57 | 2.56 | 0.22 | 2.46 | 1.09 | 0.05 | 4.11 | 4.46 | 0.19 | 1.74 | | | 99.94 |
| CAL-74 | 7995300 | 484600 | 1 | Dome | 66.64 | 15.11 | 0.69 | 2.01 | 1.77 | 3.19 | 1.33 | 0.06 | 4.09 | 4.39 | 0.25 | 0.32 | | 0.02 | 99.88 |
| CAL-133 | 7986643 | 480261 | 1 | Lava flow | 58.89 | 15.60 | 1.25 | 3.48 | 2.89 | 5.76 | 3.52 | 0.09 | 4.09 | 3.19 | 0.41 | 0.58 | | | 99.75 |

**TABLE 4. UNCALIBRATED RADIOCARBON DATES OF PEAT AND PALEOSOIL HORIZONS FROM PARICANOTA VOLCANO AREA.**

| Location and sample No. | UTM Coordinates N | E | Material | Date (yr BP)* | Stratigraphic significance | References |
|---|---|---|---|---|---|---|
| **Cotacotani Lakes** | | | | | | |
| CAL-26B | 7988845 | 474641 | Peat | 12750 ± 80 | Age of interbedded lacustrine sediments and tephra layers buried by Parinacota avalanche. | Clavero *et al.* (2002) |
| CAL-26D | 7988845 | 474641 | Peat | 11200 ± 100 | Age of interbedded lacustrine sediments and tephra layers buried by Parinacota avalanche. | Clavero *et al.* (2002) |
| CAL-26E | 7988845 | 474641 | Peat | 10550 ± 70 | Age of interbedded lacustrine sediments and tephra layers buried by Parinacota avalanche. | Clavero *et al.* (2002) |
| CAL-26G | 7988845 | 474641 | Peat | 10650 ± 80 | Age of interbedded lacustrine sediments and tephra layers buried by Parinacota avalanche. | Clavero *et al.* (2002) |
| **Near Parinacota village** | | | | | | |
| CAL-1A | 7987137 | 471631 | Paleosoil | 8600 ± 170 | Age of paleosoil horizon incorporated in Parinacota avalanche. Maximum age of Parinacota debris avalanche. | Clavero *et al.* (2002) |
| **Near Chungará Lake** | | | | | | |
| CAL-28B | 7985791 | 479091 | Paleosoil | 7790 ± 100 | Age of paleosoil horizon incorporated in Parinacota avalanche. Maximum age of Parinacota debris avalanche. | Clavero *et al.* (2002) |
| CAL-92 | 7988900 | 479750 | Peat | 8120 ± 70 | Peat layer buried by Ajata lava flow (maximum age of Ajata lava). | This study |
| **Parinacota volcano south flank** | | | | | | |
| CAL-86 | 7988100 | 484050 | Carbonised grass | Modern (<200 BP) | Carbonised vegetation buried by thin pyroclastic flow deposit. One of the youngest eruption of Parinacota volcano. | This study |

* Present is 1950 A.D.

unit) as Toreva blocks (Reiche, 1937; Figs. 3b, 5), or buried by younger flows. The remnants of the domes and the one left in place show these were thick flows, up to 150 m thick, which usually show parallel flow-banding, now tilted and dipping to the east. Their surface is usually smoothed both by glacial and alluvial erosion, but fragmented crumble breccias still remain in some outcrops. They are rhyodacitic to rhyolitic in composition (69-71% $SiO_2$, Fig. 4, Table 3) with up to 25 vol.% phenocrysts within a usually glassy matrix, which sometimes is devitrified to a perlitic and/or spherulitic texture. The phenocryst assemblage consists of quartz-plagioclase-sanidine-amphibole-biotite-sphene. Commonly the domes contain magmatic mafic inclusions with oval shapes as well as granitic and gabbroic xenoliths. Sometimes magmatic mafic bands layered with dacitic bands are found. The mafic inclusions show well-developed quenching textures with acicular amphiboles, fine-grained chilled margins and orthopyroxene phenocrysts.

Block-and-ash flow deposits are spatially and temporarily associated with the domes of the same composition, constituting their pyroclastic phase. The only in situ outcrops are located on the southern foot of the volcano (Fig. 2), and these are partly buried by Parinacota 3 pyroclastic and lahar deposits. Large volumes of these pyroclastic flow deposits form the main part of the Parinacota Debris Avalanche lower flow unit, mainly in the northern part of the deposit (Figs. 2, 3c, d). Where exposed, the individual deposits are less than 10 m thick,

have smooth surfaces and a minimum run-out of 3.5 km. They consist of a mainly monolithologic breccia, with rhyolitic (69-74% $SiO_2$, Fig. 4, Table 3) fragments up to 1 m in diameter, some of them showing well-developed PJB structures (Prismatically Jointed Blocks; Fig. 3e) and chilled margins, with glassy to microgranular textures. Clasts have a wide range of vesicularities from totally dense clasts (<1 vol.% vesicles) up to pumiceous clasts with up to 30-40 vol.% vesicles. The massive matrix is formed of fine to medium ash fragments of the same composition and is structureless. Magmatic mafic inclusions with the same petrography as those included in the domes are observed in some blocks, suggesting that magma mixing processes occurred in the magma chamber prior to eruption of these flows.

## DACITIC COULÉES AND DOMES

These flows are mainly located on the northern and south-eastern flanks of the volcano (Figs. 2, 3a, 5), partly overlain by Parinacota 3 lavas, pyroclastic flow deposits and fallout deposits. They consist of thick (up to 120 m) domes and coulées with individual lengths of up to 2.5 km. They usually have smooth surfaces mainly produced by glacial erosion with some flow ridges still preserved but buried by Parinacota 3 fallout deposits in the case of the southeastern flow. An analysis of one sample suggests they are dacitic in composition (67% $SiO_2$, Fig. 4, Table 3) with up to 20 vol.% phenocrysts. The phenocryst assemblage consists of plagioclase-sanidine-amphibole-orthopyroxene with occasional quartz, clinopyroxene and biotite.

## PARINACOTA 2 UNIT (LATE PLEISTOCENE-EARLY HOLOCENE, 70?-8 ka)

There is only one place where outcrops of lavas of this unit can be found *in situ* (avalanche scar, Figs. 2, 3a), as most of the upper part of the edifice built during this stage collapsed and formed the main body of the Parinacota Debris Avalanche upper flow unit deposit. However, some tephra fallout deposits are also preserved, interbedded with peat layers in the Cotacotani lakes area (Fig. 2). Clavero *et al.* (2002) reported four radiocarbon dates from these layers (Table 4), constraining the age of some explosive activity from Parinacota volcano during the late Parinacota 2. No reliable dates have been published so far from lavas belonging to this unit, but its age is constrained by the youngest available from Parinacota 1 unit (76.2±8.2 ka, Table 1), and the age of the Parinacota Debris Avalanche (8 ka, Clavero *et al.*, 2002). Here the authors report an age from a lava of this unit (14.1± 3.2 ka, Table 1), which suggests that Parinacota volcano had effusive activity until a few thousand years before it collapsed. Ongoing studies (B. Singer, written communication, 2004) show that eruptive activity was persistent between 40 and 15 ka. The following description summarises the observations made mainly on hummocks of the avalanche deposit, which will be later described, and on tephra fallout layers deposited in the upper Lauca basin, which were buried by the Parinacota Debris Avalanche deposit. Some original features of the lavas have also been preserved in the proximal facies of the Parinacota Debris Avalanche deposit (Fig. 6a), suggesting that the ancestral stratocone was mainly formed by Aa-type lavas interbedded with scoria fallout deposits. Two geochemical analyses obtained in this study suggest they are mainly andesitic in composition (58-62% $SiO_2$, Fig. 4, Table 3).

### LAVA FLOWS

The avalanche scar (marked S in Fig. 3a) is made of andesitic lavas, which still preserve some original features. They consist of Aa-type lava flows, up to 40 m thick with their upper surface smoothed by glacial erosion.

A few hummocks preserve the original stratigraphic and structural relations that can be attributed to Parinacota 2 lava flow domains (Fig. 6a). In these examples the lavas are typical Aa-type flows up to 20 m thick with wrinkled surfaces. Two main petrographic groups have been recognised in lavas forming the main part of the Parinacota Debris Avalanche upper flow unit. These are amphibole-rich andesites and two-pyroxene andesites. The amphibole-rich andesites contain amphibole, plagioclase and minor amounts of clinopyroxene as phenocrystic phases. The two-pyroxene andesites contain plagioclase, orthopyroxene, clinopyroxene and minor amounts of amphibole as phenocrysts.

### TEPHRA FALLOUT DEPOSITS

Fallout deposits of this unit crop out in the Cotacotani lakes area, partly buried by hummocks

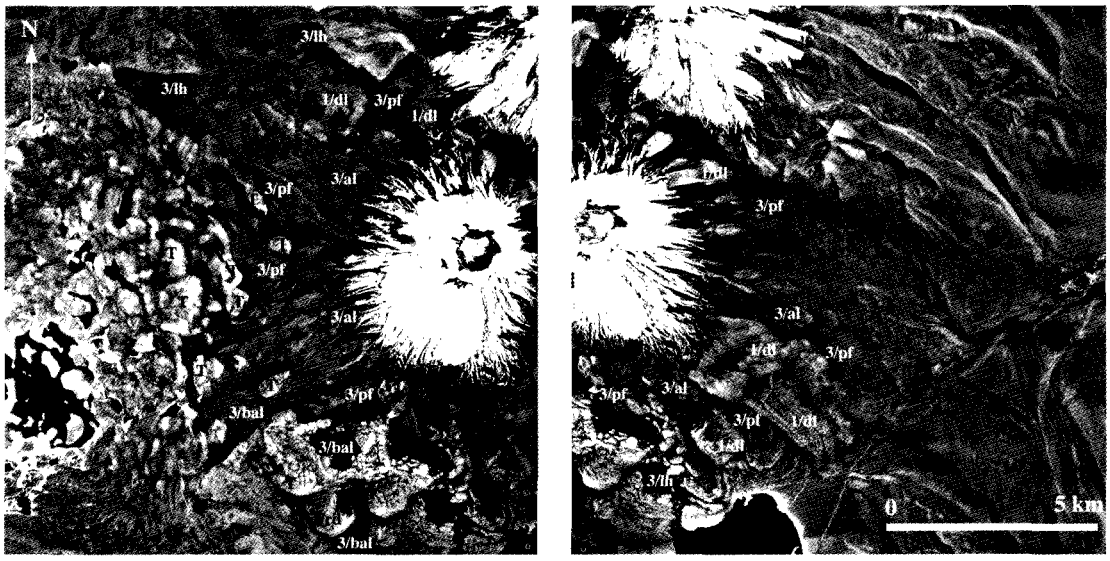


FIG. 5. Aerial photographs of Parinacota volcano showing the distribution of its different stratigraphic units; **1/dl:** Parinacota 1, dacitic lavas; **1/rd:** Parinacota 1, rhyolitic domes; **T:** Toreva blocks of Parinacota Debris Avalanche (Unit 2); **3/al**: Parinacota 3, andesitic lavas; **3/pf:** Parinacota 3, pyroclastic flow deposits; **3/lh:** Parinacota 3, lahar deposits; **3/bal:** Parinacota 3, flank cones and lavas of the Ajata centres.

of the Parinacota Debris Avalanche deposit, and, less common, in some proximal hummocks, in which primary features like original bedding have been preserved (Fig. 6a). The latter ones consist of thin (<20 cm thick) lapilli-size scoria layers (0.5-1 cm diameter) on top of lavas, which drape their irregular morphology. In the Cotacotani lakes, which correspond to kettle hole structures inside the debris avalanche deposit (Clavero *et al.*, 2002), a 5 m deep lacustrine-volcanic sequence has been exposed due to water utilization since the 1980's, which has lowered the lake levels in, at least, 5 m. The sequence consists of a series of peat, ostracod/gastropods-rich lacustrine sediments, travertine, authigenic carbonate and ash fallout layers. More detailed description and interpretation of the palaeoclimatic significance of the sedimentary deposits, were reported by Schwalb *et al.* (1999). At least six tephra fallout layers have been observed in the sequence, which consist of well-sorted thin deposits (<10cm thick), mainly formed by fine to medium ash. Clavero *et al.* (2002) reported 4 radiocarbon dates (Table 4) from this sequence ranging in age from 12,750±80 BP near the bottom to 10,650±80 BP from the top layer, showing that Parinacota 2 unit had very Late Pleistocene explosive activity. These dates are in agreement with two previously published dates from the Cotacotani lakes area by Wörner *et al.* (1988; *ca.* 13,500 BP) and Amman *et al.* (2001; 12,040±270 BP).

## PARINACOTA DEBRIS AVALANCHE (HOLOCENE, *CA.* 8 ka)

The Parinacota Debris Avalanche is a conspicuous deposit located to the west of the volcano, which marks the end of Parinacota 2 unit. It was first interpreted as a lava field by Katsui and González (1968; prior to Mt. St Helens 1980 eruption). The deposit was later reinterpreted by Francis and Self (1987), Francis and Wells (1988) and Wörner *et al.* (1988), as being a debris avalanche produced by a sector collapse. Recently, Clavero *et al.* (2002) presented a detailed investigation on the physical features of the deposit and their relation to its transport and emplacement mechanisms. Here the authors present an Ar-Ar date from a juvenile block within the deposit (7.1±3.3 ka, Table 1) that evidences a hot emplacement. The date is in complete concordance with the $C^{14}$ published age by

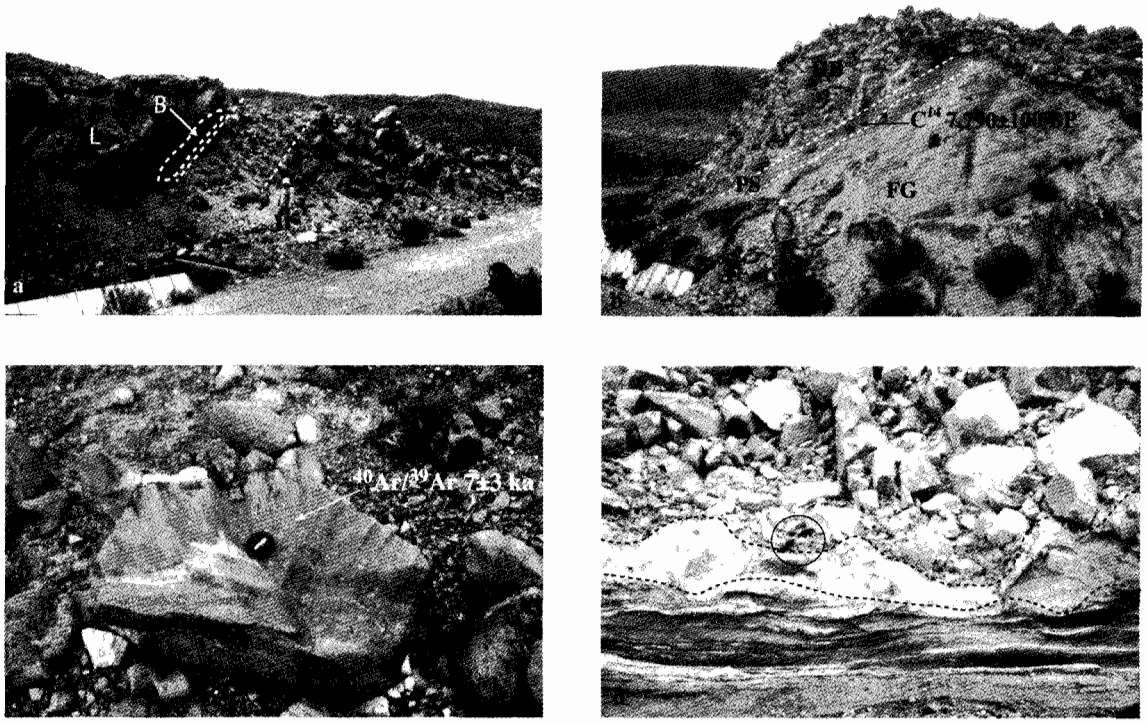


FIG. 6. Hummocks of the Parinacota Debris Avalanche deposit showing different features; **a-** original Aa-type lava flow bedding still preserved (marked with white dashed line) in proximal hummock of the upper flow unit. Note the three lavas (marked L) and the preserved brecciated base of one of them (marked B). Person for scale; **b-** original bedding in fluvioglacial and paleosoil horizons incorporated in the debris avalanche (FG and PS respectively) covered by hummock breccia (HB). A radiocarbon date ($C^{14}$ 7,790±100 BP) was obtained in the paleosoil horizon. Note person for scale; **c-** glassy dacitic PJB fragment within the Parinacota Debris Avalanche, dated (Ar-Ar) at 7±3 ka. Camera lens is 5 cm wide; **d-** lacustrine sediments near the Parinacota village, deformed and partially incorporated into the avalanche deposit, showing the structureless sedimentary basal layer of the Parinacota debris avalanche (in between the black dashed lines). Hammer in black circle for scale (25 cm in length).

Clavero *et al.* (2002). The authors summarise here, the description and key features described by these authors on the Parinacota Debris Avalanche deposit.

Around 8,000 BP, the ancestral Parinacota volcano collapsed in a single sequential catastrophic event, generating a widespread avalanche deposit to the west of the volcano. The deposit covers a minimum area of 140 $km^2$, extending to the west of the volcano, at least, 22 km (Fig. 2), with an estimated minimum volume of 6 $km^3$, similar to that suggested by Wörner *et al.* (1988). The deposit has a wedge shape, being widest near the volcano and narrowing towards the west, and displays the classic hummocky topography of volcanic debris avalanches (Ui, 1983; Siebert, 1984). A remnant of the avalanche scar can be seen on the southern flank of the volcano (Figs. 2, 3a). Minimum velocities were estimated for the flow at 60 m/s, 12 km from the source, and 25 m/s near the end of the deposit. The deposit consists of two flow units with different compositions and morphologies (Fig. 2).

The lower flow unit is divided itself into two subunits. One subunit consists of large Toreva blocks of rhyolitic to rhyodacitic domes that crop out in the proximal facies of the deposit (Figs. 3b, 5), corresponding to large tilted blocks of the original edifice that slid and came to rest at the foot of the volcano. The other subunit is composed mainly of rhyolitic to rhyodacitic block-and-ash flow deposits and breccias of flow banded rhyolite and dacitic lava flows, and minor fluvioglacial deposits (Figs.

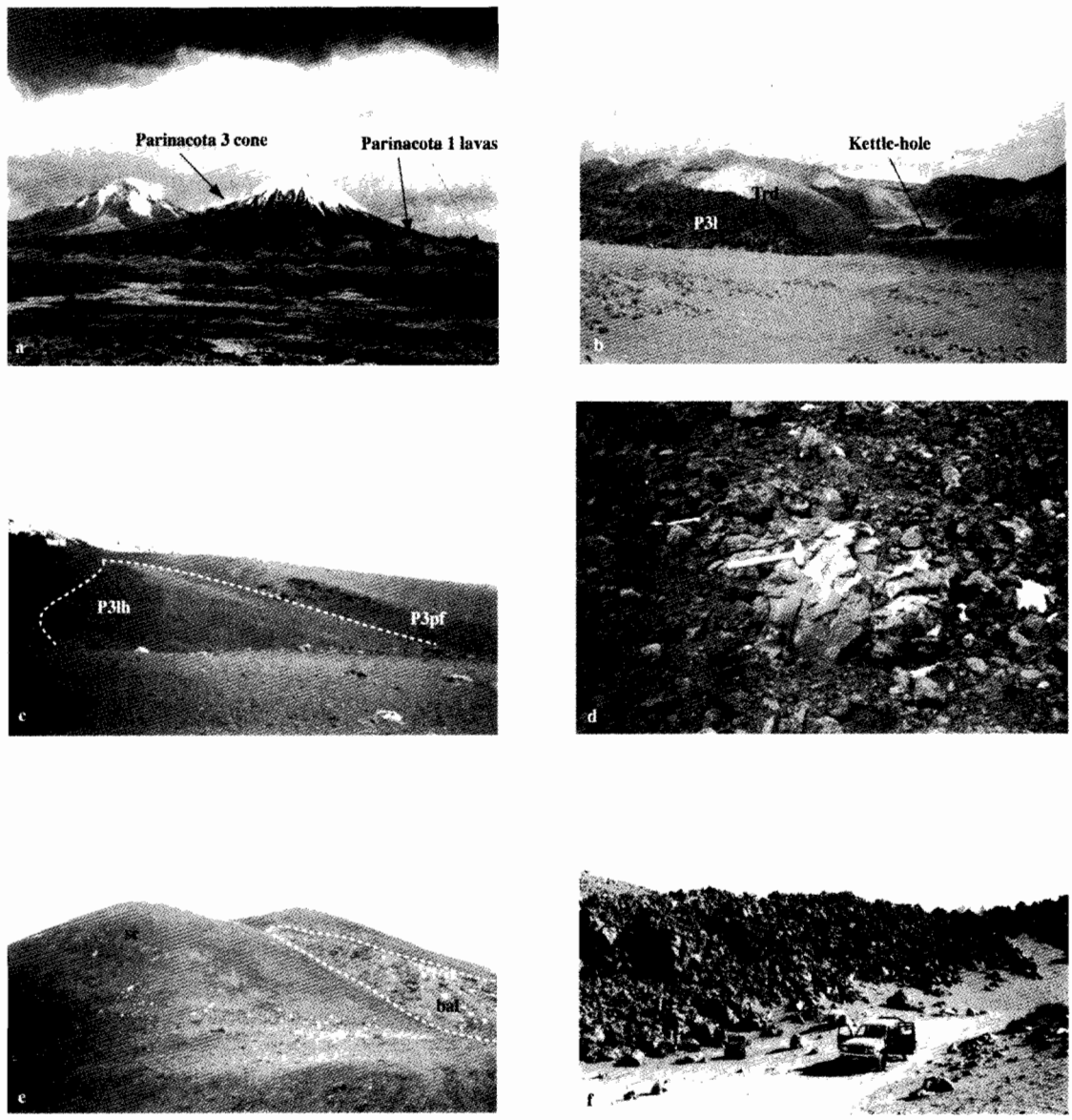


FIG. 7. **a-** Parinacota volcano viewed from the south-west showing the new cone built during the Holocene on top of the remnants of the ancestral Parinacota volcano (Parinacota 1 lavas); **b-** western foot of Parinacota volcano viewed from the north-east. Kettle-hole structures of the Parinacota Debris Avalanche are observed surrounded by Toreva blocks (Trd) and partially filled by Parinacota 3 andesite lavas (P3l); **c-** western foot of Parinacota volcano viewed from the north. A welded Parinacota 3 pyroclastic flow deposit (P3pf) can be seen cut and partially covered by Parinacota 3 lahar deposits (P3lh); **d-** detail of a breadcrust scoria bomb on top of a Parinacota 3 pyroclastic flow deposit. Hammer is 30 cm in length; **e-** southern Ajata centre formed by a scoria pyroclastic cone (sc) with its associated basaltic andesite lava flow (bal); **f-** southernmost lava flow from the Northern Ajata centres showing its typical Aa morphology.

3c, d, 6b). This subunit shows a smooth undulating morphology with numerous low amplitude hummocks (Fig. 3c). Well-preserved PJB fragments are common in this subunit, and two kinds of them have been recognised so far. They form block domains within the deposit, being the most common (Fig. 3e) petrographically, geochronologically (Table 1) and geochemically (Table 3) identical to rhyodacitic block-and-ash flow deposits. These domains are interpreted as being Parinacota 1 deposits

incorporated by the avalanche during the collapse. The other block domain corresponds to glassy dacitic (Table 3) PJB fragments (Fig. 6c), of which very few have been found so far. Thus, the occurrence of these dacitic PJB fragments, is interpreted to be representative of a cryptodome intrusion that probably helped to trigger the collapse of the edifice as it will be discuss later.

The upper flow unit is predominantly composed of andesitic lava domains, ranging from coherent blocks to hummocks made of breccia, containing little or no matrix at all, with the exception of a structureless sedimentary basal layer (Fig. 6b, 6d). The rock types range from basaltic andesite to dacite, with two-pyroxene andesite and amphibole-rich andesite being dominant. This unit displays pronounced hummocky topography, in which hummock volume and amplitude decrease with distance and towards the margins of the deposit.

### PARINACOTA 3 UNIT (HOLOCENE, <8 ka)

It corresponds to a sharply defined stratocone (Figs. 3a, 7a) that includes a series of lavas and pyroclastic flow deposits radially distributed around the cone (Figs. 2, 5). Tephra fallout deposits, mainly directed towards the east according to the predominant high wind direction are also part of this unit. This activity was sourced mainly at a central summit vent, and has been accompanied by the generation of lahars and by formation of a series of flank cones and their associated lava flows (Ajata centres; Figs. 2, 7e, 7f). The construction of this new cone, which has probably continued until recent times, formed an almost perfect conical-shaped stratovolcano with an estimated minimum volume of 18 km3 (Figs. 3a, 7a). Only one reliable date has been published from a lava of the main central new cone (Wörner *et al.*, 2000a), giving an age of 1,660±350 BP (He-exposure age). This is in agreement with Clavero *et al.* (2002) who suggested that the new cone was completely built during the Holocene, based on the age of the Parinacota Debris Avalanche.

#### LAVA FLOWS

These lavas form the main part of the new cone and are interbedded and partly covered by tephra fallout, pyroclastic flow and lahar deposits of the same unit, and covered by a permanent ice cap (Jordan, 1999) on the upper part of the cone (Fig. 5). These flows were emplaced and almost completely overflowed the Parinacota Debris Avalanche scar, whose only remnant can be seen on the southern flank of the volcano (Fig. 3a). The lava flows are distributed all around the volcano and mainly consist of aa-type lava flows with thickness ranging from 10 to 40 m, reaching distances of up to 7 km from their source (Fig. 7b). They are commonly a few hundreds of metres wide, but some distal lobes of the lowermost western flows are up to 1,200 m wide (Fig. 2). They have very well preserved primary morphologies, like levées, flow ridges and lobes.

The lavas are essentially andesitic in composition (58-60% $SiO_2$, Fig. 4, Table 3), and mainly consist of two-pyroxene andesites with minor amounts of amphibole and olivine phenocrysts.

### FLANK CONES AND LAVA FLOWS (AJATA CENTRES)

These parasitic centres are located on the south-western flank of Parinacota volcano (Figs. 2, 5). They can be divided into two groups according to their geographic locations, the northern and southern Ajata centres, equivalent to the 'High Ajata' and 'Upper and Lower Ajata', respectively of Entenmann (1994) and Wörner *et al.* (2000a). The source fissures for both groups are aligned in NNE and NS direction, respectively (Fig. 2).

#### NORTHERN AJATA CENTRES

The northern group consists of a series of at least four different emission centres and at least five associated lavas flows. The NNE alignment of centres is parallel to the regional Parinacota-Condoriri lineament (Fig. 2). At least one emission centre, from which the northernmost lava flow originated, is overlain by younger lahar and pyroclastic flow deposits. These emission centres consist of small pyroclastic cones, up to 150 m in diameter and 60 m high (with crater up to 50 m in diameter and 20 m deep). The lavas were directed mainly to the south and west, reaching distances of up to 3 km from their origin. The northernmost one shows well-preserved levées, flow ridges and developed three distinct lobes in its final stage. Its width reaches more than 1,000 m. It has a typical aa morphology with a thickness of up to 20 m (Fig. 7f).

These flows can be divided into two groups according to their chemical composition and mineralogy. The northern one is andesitic in composition with up to 15 vol.% phenocrysts, mainly corresponding to plagioclase, clinopyroxene, orthopyroxene and minor amounts of olivine, which means it is very similar to the lavas erupted from the main cone. The southern lavas of this group are identical petrographically and geochemically to those erupted from the southern Ajata centres, which will be later described. According to the geochronologic data published by Wörner *et al.* (2000a), this group is the youngest of the Ajata centres (He-exposure ages ranging from 1,385±350 BP to 2,160±280 BP). The authors present here one radiocarbon date from a peat layer buried by the lava (Table 4), which gives it a maximum age of 8,120±70 BP, in agreement with the previously published dates.

## SOUTHERN AJATA CENTRES

The southern group consists of two pyroclastic cones and at least four different lavas, mainly directed towards the south (Figs. 2, 5). The pyroclastic cones have subcircular basal shapes with diameters up to 250 m and heights up to 70 m (Fig. 7e). The southern one has a breached crater (100 m in diameter and 15-20 m deep) towards the east from which a lava flow formed (Fig. 7e). The lavas have very well preserved primary features like levées, flow ridges and lobes. They have typical Aa morphologies with a maximum thickness of 20 m and a maximum width of 1,300 m. The southernmost lava almost reached the Chungará Lake (Fig. 3a). The lavas consist of basaltic andesites (Entenmann, 1994), mainly aphyric, in places highly vesicular, with less than 5 vol.% phenocrysts, mainly olivine, clinopyroxene, orthopyroxene and minor amounts of plagioclase. According to Entenmann (1994) plagioclase and sanidine xenocrysts are common, as well as some amphibole phenocrysts with thin to thick opacitic rims. A more detailed description of the chemical compositions of these flows was given by Entenmann (1994). Wörner *et al.* (2000a) published three dates (He-exposure ages) from these flows ranging in age from 6,560±1220 BP for the southernmost one to 3,050±450 BP for the central one.

## PYROCLASTIC FLOW DEPOSITS

These deposits are located all around the lower flanks of the volcano, and are interbedded with lavas of the main new cone (Parinacota 3; Figs. 2, 5). One of these pyroclastic flow deposits overlies the northernmost lava flow of the Ajata centres, which is the youngest eruptive product of the parasite centres (Wörner *et al.*, 2000a). These small-volume pyroclastic flow deposits are commonly poorly consolidated, but in some cases are strongly welded with well-developed fiamme and eutaxitic textures. Their maximum runout is 7 km from the central vent and their thickness varies from tens of centimetres up to 30 m in the most proximal facies, on the southern flank of the volcano. Their morphologies vary from ones being smoothed and cut by laharic erosion (Fig. 7c) to others unaffected by erosion, with very fresh surfaces, well-preserved dendritic lobes (Fig. 5) and abrupt flow fronts. They consist of poorly sorted breccias with breadcrust bombs up to 2 m in diameter (Fig. 7d) within a fine to medium grained matrix formed by juvenile material (90%) and accessory fragments (mainly Parinacota 2 lavas).

The juvenile fragments are usually texturally and compositionally banded. The texture bands are mainly due to different vesicularities, and the composition bands are due to magma composition variations (andesitic and dacitic). The juvenile clasts that are not compositionally banded include both scoria and pumice with andesitic and dacitic compositions, respectively (Fig. 4, Table 3).

Scoria fragments have similar mineralogy to Parinacota 3 main cone lava flows. They consist of plagioclase, clinopyroxene and orthopyroxene phenocrysts within a usually highly vesicular groundmass. In some cases the mafic bands within the juvenile material show similar quenching textures to those found in Parincaota 1 mafic inclusions. Pumiceous clasts consist of plagioclase, clinopyroxene, orthopyroxene and amphibole phenocrysts within a highly to moderately vesicular groundmass with different textures and are similar petrographically and geochemically to Parinacota 2 lavas.

The authors report a date obtained in Parinacota 3 pyroclastic flow deposits. It consists of a radio-

carbon date from grass buried and slightly burned by a fresh-looking pyroclastic flow deposit on the southern flank of the volcano. The result gave a 'modern age' (Table 4), which indicates that it is younger than 200 years BP (laboratory limit).

## TEPHRA FALLOUT DEPOSITS

These deposits are mainly located towards the east of the volcano and can be found as far as 15 km from the volcano in Bolivia, although thin layers can also be found close to the western flank of the volcano. They overly Parinacota 3 pyroclastic flow deposits and lavas, as well as older units (Fig. 2). They consist of well-sorted deposits that are usually spatially and temporarily associated to Parinacota 3 pyroclastic flow deposits, and their petrography and chemical composition are identical to the juvenile material. Their thicknesses vary from less than a centimetre up to 20 cm close to the volcano, with fragment size variations from fine ash to medium lapilli, from distal to proximal areas. Their spatial and compositional relationships with Parinacota 3 pyroclastic flow deposits, which are similar in extension and volume to the pyroclastic flows generated by the eruption of Láscar volcano in 1993 (Gardeweg *et al.*, 1998), suggest that most of these deposits correspond to sub-plinian style explosions associated to the generation of the pyroclastic flows.

## LAHAR DEPOSITS

Lahar deposits are located all around the volcano with the exception of the northern flank, where no major gullies are developed (Figs. 2, 5). The maximum runout is 8 km from the source (lower edge of Parinacota Glacier limit), forming the northwestern fan between Parinacota and Pomerape debris avalanche deposits (Figs. 2, 5). The individual flow deposit thicknesses vary from 20 cm up to 1 m. The deposits consist of polylithologic breccia deposits, with subangular to subrounded fragments up to 3 m in diameter, mainly from Parinacota 3 lavas and pyroclastic flows. The matrix is commonly medium grained sand made of rounded to subrounded fragments with abundant pores and well to poorly developed bedding. Their surfaces are usually flat and they commonly overly and cut both lavas and pyroclastic flow deposits of Parinacota 3 unit as well as older units (Figs. 2, 5, 7c).

## LEGENDS AND VOLCANIC ACTIVITY

Local legends, myths and historical records can be very helpful to interpret the recent volcanic activity of volcanoes. Such interpretations have been recently used for instance to reconstruct the eruptive history of some volcanoes of the southern Andes in the last 440 years, since the first Spanish conquerors arrived at the area (Petit-Breuilh and Lobato, 1994; Petit-Breuilh, 1999).

In the case of Parinacota volcano area the first Spanish conquerors probably arrived around 460 years ago, but they only started to colonise the Altiplano of Northern Chile in the Late XVII to Early XVIII century, building the first churches in the Aymara (local pre-hispanic inhabitants of the Altiplano of Chile, Bolivia and Peru) region. No historical records of eruptive activity associated to Parinacota volcano have been found so far from Spanish accounts. However, a series of Aymara myths and legends involving the volcanoes of the area exists. Here, the authors briefly describe one of these legends that is relevant to the possible eruptive activity of Parinacota volcano in recent times.

## THE BEARDED MAN AND THE CATASTROPHE

'Originally the Chungará area was an extremely grass-rich bofedal (water meadows or soligenous peatland) where a healthy village was located. Some day, while having a huge party, a bearded beggar asked for food and drink to the local Cacique (Head of the village or area). This created a strange feeling in the community as the Aymaras are usually beardless, but everybody forgot that a hirsute beard characterises the Sun's son, Wiracocha. But the Cacique treated the beggar very rudely, ordering him to leave the area. However, the beggar could make his way to the kitchen where a woman and her son fed him. A few weeks later, the beggar revealed as a divine messenger and told the cook and his son that a great misfortune was about to take place and they should leave immediately the area without looking back. While leaving the area, near Tambo Quemado (Burned Tambo in Spanish), her curiosity was so big that she turned around. A huge fire was falling on

the bofedal, with such a high intensity that it even burned the water. An apocalyptic smoke came from the earth all around the region. The fire consumed the village of Lakhata (burned in Aymara).'

This legend has been interpreted by journalists (El Mercurio, April 2000) as being related to the origin of the Chungará Lake. However, the Chungará Lake formed *ca.* 8,000 years ago, when the Parinacota Debris Avalanche dammed the Upper Lauca basin. Therefore, the legend cannot be attributed to that event, as the Aymaras have not such a long history, and by the time the ancestral Parinacota volcano collapsed, the major human settlements were located on the coast and consisted of very primitive tribes. On the other hand, the legend clearly says that the eruption entered and burned the water, indicating that the Chungará Lake was already formed. Considering that the Aymaras have been living in the Altiplano since *ca.* 1,000-1,500 years ago (after the last documented eruption of the Ajata centres), the authors suggest that the legend refers to a very recent eruption of Parinacota volcano. The influence of biblical stories (Lot's wife looking back at Sodom's destruction was converted in stone) in the legend suggests, on the other hand, that it started after the first conquerors and, of course, evangelists passed through Aymara land. These interpretations, added to the 'modern age' of a pyroclastic flow deposit in the southern flank of Parinacota volcano, make very likely that its last eruption occurred at some point in the lateXVII early XVIII century and generated a small-volume pyroclastic flow directed to the south, whose ash clouds probably reached the original village and entered the Lake.

## GEOCHEMISTRY

In this section, the autors briefly summarise the results from the detailed studies on Parinacota volcano geochemistry and petrology published by Wörner *et al.* (1988, 1992a, b, 2000a); Davidson *et al.* (1990); Entenmann (1994) and Bourdon *et al.* (2000), and the authors add their new data from major element analyses, which are listed in table 3 and shown in figure 4.

During Parinacota 1 unit a geochemically wide range of magmas was erupted (59-74% $SiO_2$, Fig. 4). Wörner *et al.* (1988) interpreted these rocks as showing a well-defined crystal fractionation trend, similar to those observed on other high-K calc-alkaline volcanic series. During Parinacota 2 unit only andesitic magmas were erupted (57-63% $SiO_2$); although this narrow range could also be due in part to difficulties in finding rocks of this unit. After the collapse of the ancestral stratovolcano, the composition of the magmas varied from basaltic andesites (53% $SiO_2$) to dacites (64% $SiO_2$), with the most mafic ones only erupting from the Ajata centres. In general terms, the chemical composition of the magmas erupted from the main vent during Parinacota 3 unit is slightly more mafic than those erupted prior to the collapse, although some amphibole-bearing silicic andesitic and dacitic bombs are common in the pyroclastic deposits, suggesting that some batches of 'older' magma still remained in the system.

One of the most striking features is the high Ba and Sr content relative to other volcanic centres of the Central Andes. The decrease of Ba content with increasing silica content has been interpreted by Wörner *et al.* (1988) and Davidson *et al.* (1990) as the result of alkali feldspar crystallisation; and the isotope compositions suggest, on the other hand, a complex magma genesis. These authors, based on these isotopic characteristics, suggested that the parental magmas of the Nevados de Payachata Volcanic system (Parinacota and Pomerape volcanoes) have been produced by deep mixing between primary subcrustal and lower crustal components, which further differentiated in upper crustal chambers through combined processes (fractional crystallisation, assimiliation, magma mixing).

## DISCUSSIONS

The volcanic evolution and stratigraphy of Parinacota volcano have important implications for the evolution and behaviour of Central Andes stratovolcanoes, for the assessment of volcanic hazards of one of the biologically richest areas of the High Andes, and for the late Quaternary history of this part of the Altiplano.

### VOLCANIC EVOLUTION

Based on the new mapping and geochronological data, a new three-stage volcanic evolution for Parinacota volcano is proposed. In table 2, this scheme is compared with the previous ones by Katsui and González (1968) and Wörner *et al.* (1988). The detailed information now available on the Parinacota Debris Avalanche (Clavero *et al.*, 2002) has also been crucial to better understand the evolution of the first stages of Parinacota volcano. The debris avalanche was produced by a sequential collapse during a single catastrophic event of the ancestral volcano and its flow units preserved the original stratigraphic relationships (Clavero *et al.*, 2002). The lower flow unit consists only of rocks from the earliest stage of Parinacota volcano, whereas the upper flow unit consists only of andesitic lava flow fragments, which formed a stratocone built on top of the previous complex.

The authors will now mainly compare their scheme to Wörner *et al.*'s (1988) as this scheme differs only slightly from that of Katsui and González (1968), and also because the older scheme was proposed prior to the recognition of the Parinacota Debris Avalanche deposit and without geochronologic data. The authors' model differs from Wörner *et al.*'s (1988) as follows: as suggested by Wörner *et al.* (1988) Parinacota volcano started to build around 300 ka ago with the effusion of a series of andesitic lava flows (Stage Ia from Wörner *et al.*, 1988; Table 2). The authors also include in this first stage (Unit 1 in the authors' scheme, Table 2, Fig. 8a) dacitic lava flows that are spatially associated to the andesites, which were also incorporated in the Parinacota debris avalanche lower flow unit. These flows were included in Stage II by Wörner *et al.* (1988), but fragments of these rocks are not found in the debris avalanche upper flow unit, which is mainly formed by Parinacota 2 unit fragments. The same authors suggested that the effusion of these andesitic lava flows was followed by the formation of a rhyolitic dome complex and its associated block-and-ash flow fans (Stage Ib from Wörner *et al.*, 1988; Table 2). The authors propose that the formation of the rhyodacitic-rhyolitic dome complex and the effusion of the andesitic lavas were contemporaneous events (Fig. 8a, 8b). The geochronologic data suggest there were probably two distinctive eruptive phases, with the effusion of rhyolites and andesites simultaneously during each period. The oldest phase probably occurred at around 260-300 ka, and the youngest at around 110-70 ka (Fig. 8a, b). Unfortunately, no radiometric dates have yet been obtained from the dacitic coulées. Their spatial distribution (Figs. 2, 3a), however, suggests they were probably erupted contemporaneously with the youngest rhyodacitic domes and andesitic lava flows at around 110-70 ka. More geochronologic investigations will be needed, however, to better understand if Parinacota 1 edifice was built in two different phases or continuously from 300 ka to 70 ka, or even younger.

During the second stage (Parinacota 2 unit; 70?-8 ka) a stratocone was built on top of the rhyolitic-andesitic lava-dome complex (Fig. 8c). This ancestral Parinacota stratocone was mainly formed by andesitic lava flows as can be deduced from the rocks forming the main body of the Parinacota Debris Avalanche upper flow unit and the avalanche scar. There is no evidence that more silicic products were erupted during this stage as proposed by Wörner *et al.* (1988). These authors also proposed, and subsequent studies assumed (Davidson *et al.*, 1990; Wörner *et al.*, 2000a; Bourdon *et al.*, 2000), that Parinacota volcano collapsed due to a Mount St. Helen's type eruption, triggered by a cryptodome intrusion, which formed a dacitic plinian fallout deposit, but where evidence of a blast deposit lacks. As described earlier, rhyodacitic PJB are common in the Parinacota Debris Avalanche deposit, which come from Parinacota 1 deposits incorporated into the avalanche. Glassy dacitic PJB are rare in the deposit. The consistent age (Table 1) of the last ones with the age of the debris avalanche suggests they could correspond to fragments of a cryptodome

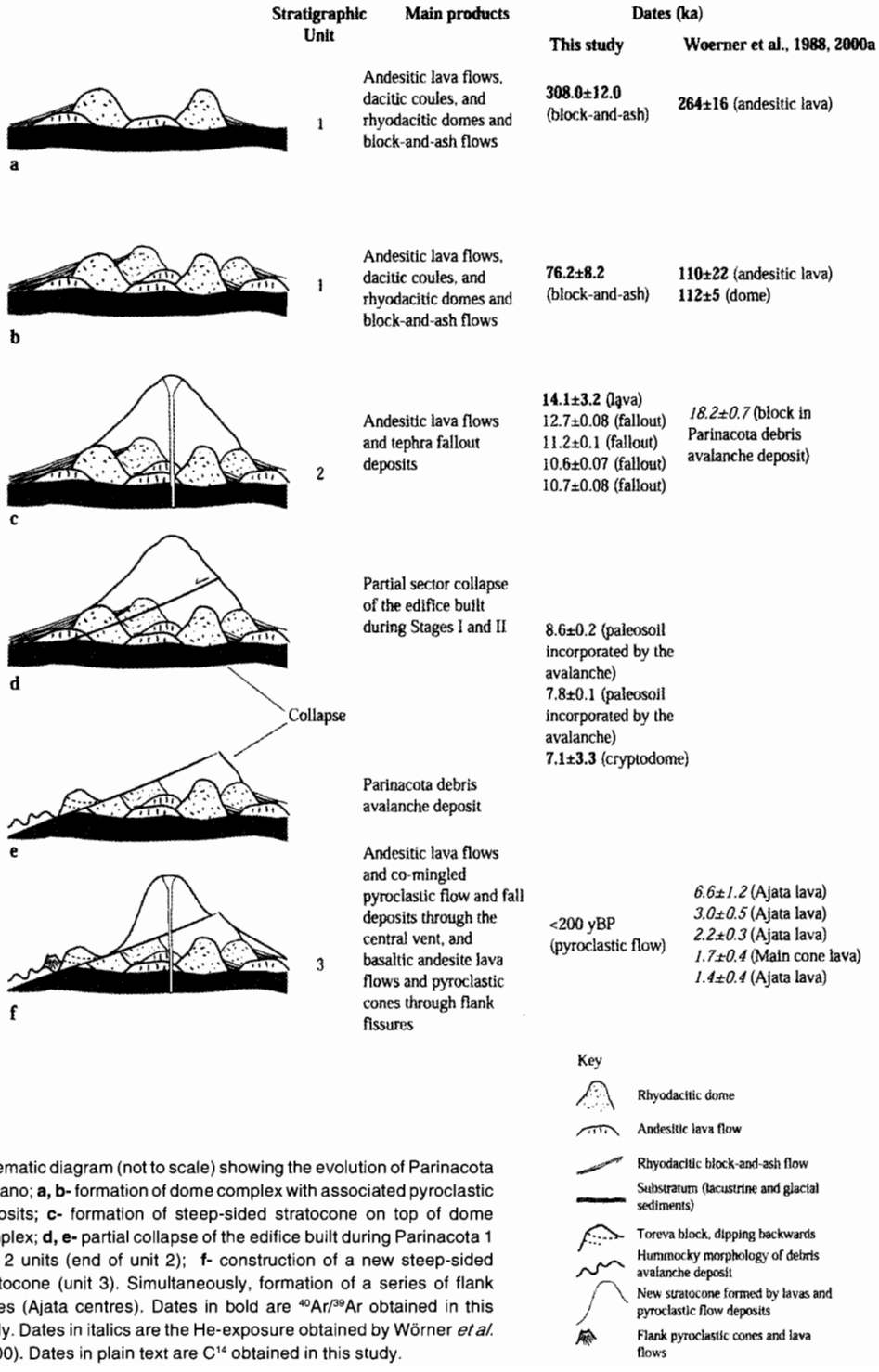


FIG. 8. Schematic diagram (not to scale) showing the evolution of Parinacota volcano; **a, b-** formation of dome complex with associated pyroclastic deposits; **c-** formation of steep-sided stratocone on top of dome complex; **d, e-** partial collapse of the edifice built during Parinacota 1 and 2 units (end of unit 2); **f-** construction of a new steep-sided stratocone (unit 3). Simultaneously, formation of a series of flank cones (Ajata centres). Dates in bold are $^{40}Ar/^{39}Ar$ obtained in this study. Dates in italics are the He-exposure obtained by Wörner *et al.* (2000). Dates in plain text are $C^{14}$ obtained in this study.

that helped to trigger the sector collapse of the ancestral edifice (Fig. 8d, e).

Soon after sector collapse, a new stratocone started to build with the extrusion of slightly more mafic magmas generating lava flows and pyroclastic flows and tephra fallout (Fig. 8f). This explosive activity, represented by the pyroclastic flows and tephra fallout, has been very important in recent times. Most of the pyroclastic deposits show strong evidence of magma mixing processes (banded and two chemically different juvenile material) that occurred in the magma chamber prior to the eruptions. Replenishment of the magma chamber is likely to have triggered some explosive eruptions, as has been suggested for numerous eruptions worldwide (Sparks *et al.*, 1977; Pallister *et al.*, 1992; Naranjo, 1992; Naranjo *et al.*, 1993; Murphy *et al.*, 2000). Wörner *et al.* (1988) and subsequent authors (Davidson *et al.*, 1990; Entenmann, 1994; Bourdon *et al.*, 2000) have interpreted the flank cones and lava flows (Ajata centres) as being the youngest products and evolution stage of Parinacota volcano (Table 2). Based on the He-exposure dates from Ajata lava flows (ranging between 6 and 1.4 ka, Wörner *et al.*, 2000a), with the authors' new mapping and geochronologic data ($C^{14}$ and $^{40}Ar/^{39}Ar$), it is now clear that these centres have been active simultaneously with the formation of the main cone (Fig. 8f). On the other hand, the authors report here new evidence ($C^{14}$ date, Table 4) suggesting that Parinacota volcano last eruption generated a pyroclastic flow directed to the south, probably during historical times (see legend and volcanic activity chapter).

## GEOCHEMISTRY

The main aim of this work has been to better understand the volcanic evolution of Parinacota volcano. Here the authors discuss a few geochemical aspects on this evolution, but do not discuss the main petrological-geochemical results obtained by previous authors in the area which are based on much more detailed geochemical studies (Wörner *et al.*, 1988; Davidson *et al.*, 1990; Bourdon *et al.*, 2000).

Wörner *et al.* (1988) found rare petrographic evidence for magma mixing, which is suggested to have occurred based on geochemical data (*i.e.*, Ni-Rb variations) and, therefore, interpreted these processes to have led to a complete rehomogenization of magmas. They conclude then, that magma mixing was not a short-term pre-eruptive process. However, their observations (mafic inclusions, bimodal juvenile composition in pyroclastic deposits, etc.) support that magma-mixing has been probably recurrent during Parinacota 3 unit, but also that they were probably short-term pre-eruptive processes and possibly explosive triggering mechanisms (Sparks *et al.*, 1977).

Recently, Bourdon *et al.* (2000) based on U-series investigations, proposed some time constraints on magma differentiation for Parinacota volcano. They obtained three U-Th dates from different rocks of Parinacota volcano. One of them, from a rhyolitic dome, gave a U-Th age (92.2±2.3 ka), which is younger than the eruption age (K-Ar 112±5 ka, Wörner *et al.*, 1988). One sample from an Ajata flow gave a U-Th age older (26.5±6.6 ka) than the eruption age (He-exposure age of 6.3±0.7; Wörner *et al.*, 2000a), which was interpreted to be the reflect of phenocrysts residence times in the magma chamber prior to the eruption. The last sample these authors analysed was a dacitic block within the Parinacota Debris Avalanche deposit, which they interpreted as primary magma that triggered the eruption. This sample gave a much older U-Th age (123.5±2.7) than the interpreted eruption age (He-exposure age of 18.1±0.6 ka, Wörner *et al.*, 2000a), and thus, the authors interpreted it as being representative of phenocrysts long residence times in the magma chamber (*ca.* 100 ka) prior to the eruption. However, the block dated by Bourdon *et al.* (2000) and interpreted as reflecting the new magma that triggered the eruption of the Parinacota Debris Avalanche, is dacitic in composition and the block from which a He-exposure age was obtained (Wörner *et al.*, 2000a), also interpreted as being representative of the new magma that triggered the eruption, is andesitic in composition. Thus, both samples dated by different methods (U-Th and He-exposure) correspond to samples from different stratigraphic units. On the other hand, the age of the dacitic block is consistent with Parinacota 1 rhyodacitic domes and block-and-ash flow deposits (Wörner *et al.*, 1988), which form the main body of the Parinacota Debris Avalanche lower unit deposit, some of which still preserve primary PJB structures. Thus, at least another interpretation can also account for this

older U-Th age. This is to consider the U-Th age to be representative of the eruption age (*ca.* 125 ka) and then interpret the block as part of Parinacota 1 unit (from a block-and-ash flow deposit) and incorporated later into the Parinacota Debris Avalanche deposit. One way to discriminate between these two interpretations, would be to look at the chemical composition of the block dated by U-Th, as the cryptodome has a dacitic composition (63% $SiO_2$, Table 3) whereas Parinacota 1 block-and-ash flow fragments have rhyodacitic compositions (68-72% $SiO_2$, Table 3).

## AGE AND ORIGIN OF THE PARINACOTA DEBRIS AVALANCHE

Wörner *et al.* (1988) were the first authors to suggest a Late Pleistocene age (minimum age of *ca.* 13,500 BP) for Parinacota debris avalanche, based on a $C^{14}$ date obtained by P.W. Francis in peat layers located in the Cotacotani lakes area (Fig. 3). Wörner *et al.* (2000a) presented a He-exposure date obtained in an andesitic (see Wörner *et al.*, 1988) columnar jointed block left exposed by the collapse, which gave an age of 18,150±650 BP. They interpreted it as a magmatic primary block, and, therefore, as giving the age of the collapse. Recently, Clavero *et al.* (2002) presented new $C^{14}$ data of both peat layers from the Cotacotani lakes area, and palaeo-soil horizons incorporated in the debris avalanche deposit (Table 4, Fig. 8b). These data show that the collapse occurred at *ca.* 8 ka BP. The sediments now outcropping in the Cotacotani lakes area deposited in a large lake basin located in the Upper Lauca basin prior to the collapse and were partly buried by the avalanche deposit. They are now exposed due to the formation of large kettle hole structures within the deposit. The block dated by Wörner *et al.* (2000a) is interpreted here as corresponding to a Parinacota 2 unit andesite erupted or left exposed to the atmosphere *ca.* 10 ka prior to the collapse, which was afterwards incorporated into the avalanche.

Clavero *et al.* (2002) showed that Parinacota volcano was built on top of lacustrine deposits of the Lauca basin, which was partly infilled by wet lacustrine, pyroclastic and glacial deposits (Fig. 9a). They proposed that the loading effects of the construction of a dense edifice on top of this ductile substratum might have caused its deformation and the consequent spreading of the edifice. Loading of wet sediments is thus a plausible primary cause for the volcanic edifice to collapse and form the debris avalanche. This loading triggering mechanism for generating edifice collapses has been widely investigated in recent years both by analogue experiments and field research (Borgia, 1994; Van Wyk de Vries and Borgia, 1996; Merle and Borgia 1996; Van Wyk de Vries and Francis. 1997; Van Wyk de Vries and Matela, 1998). This mechanism has been suggested to be the main cause of the edifice failure, which generated the Socompa debris avalanche (Van Wyk de Vries *et al.*, 2001). The deformation of Parinacota volcano substratum could have also been accompanied by some deformation of the edifice itself (Fig. 9a). The occurrence of NNE and NS fissures (normal to the collapse direction and subparallel to major extensional faults located in the Condoriri Volcanic Complex area and to the Parinacota-Condiriri lineament, Fig. 3) suggests that some almost east-west extension might have occurred in the edifice prior to the collapse. These fissures were used again by magmas to erupt, after the collapse, forming the Ajata centres. It has been suggested that magmas commonly reuse fissures (or feeder conduits) many times to rise to the surface (Hildreth and Moorbath, 1988). This fact can be observed in Parinacota volcano as the same couple of fractures have been used several times, at least during 4.5 ka to form the Ajata flank centres. If these magmas reached the surface reusing old conduits, it is then very likely that east-west extension occurred in the edifice prior to its collapse. Extension normal to the collapse direction of edifices due to dyke intrusions or rift zones has been observed or modelled in many volcanoes (Siebert *et al.*, 1984; Lipman *et al.*, 1985; Moore *et al.*, 1989; Voight and Elsworth, 1997; Hürliman *et al.*, 2000). In some cases dyke intrusion and earthquakes are interpreted to be the primary cause of flank failures (Elsworth and Voight, 1995; Day *et al.*, 1997; Elsworth and Day, 1999) (Elsworth and Voight, 1995). Another factor, but not least important, that might have caused some deformation of the edifice and probably finally triggered its failure, was the intrusion of a dacitic cryptodome. Evidence for the existence of this cryptodome is the occurrence of some glassy dacitic (63% $SiO_2$) PJB fragments of *ca.* 7 ka (Table 1) within the debris avalanche deposit. The intrusion of this viscous magma in the

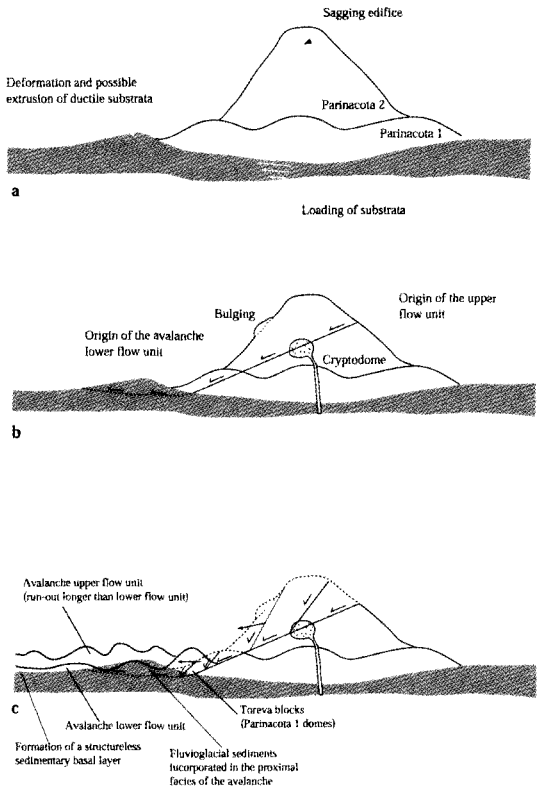


FIG. 9. Schematic diagram (not to scale) showing the ancestral Parinacota volcano prior (a), during (b) and after (c) the collapse that generated the Parinacota debris avalanche deposit; **a-** sagging of the ancestral edifice due to the deformation of the ductile substrata because of loading; **b-** intrusion of a cryptodome, deforming (bulging) the edifice. Collapse of the edifice caused by several factors (bulging, loading of ductile substrata and deformation by dyke intrusion). Possibly one of the wet sedimentary layers acted as the final décollement plane; **c-** deposition of the Parinacota debris avalanche deposit, and formation of the two distinctive flow units, preserving the original stratigraphy of the ancestral edifice (the lower one, with less energy coming to rest near the foot of the volcano; and the upper one, with higher energy, reaching longer distances from the volcano). Incorporation of some of the sedimentary layers in the proximal areas of the avalanche deposit.

edifice probably produced its bulging (Lipman *et al.*, 1981) and final sequential collapse (Fig. 9b, c), but unlike Mount St. Helen's eruption, there is no evidence that the collapse was followed by a blast (Voight *et al.*, 1981; Hoblitt *et al.*, 1981).

## MAGMA PRODUCTIVITY

No reliable estimation of magma productivity can be estimated for the first two units of Parinacota volcano, until further geochronological data are obtained.

However, the very high eruption rate during Parinacota 3 unit (>2.25 $km^3$ $ka^{-1}$ or >2.25x$10^{-3}$ $km^3$ $y^{-1}$), makes it one of the most active volcanoes of the Central Andes during the Holocene (Crisp, 1984; de Silva and Francis, 1991; Francis and Hawkesworth, 1994), even more active than Láscar volcano (*ca.* 1 $km^3$ $ka^{-1}$), which has been considered the most active volcano in northern Chile (Gardeweg *et al.*, 1998). This value is comparable to the effusion rate of other active volcanoes around the world, which have erupted through much thinner crusts, considering similar periods of time, like Oshima and Sakurajima in Japan, Fuego in Guatemala, Avachinsky in Russia (Crisp, 1984) and Santorini in Greece (Druitt *et al.*, 1999). The effusion rate of Parinacota volcano in the Holocene is equivalent to that obtained for all the active volcanoes of the Central Andes (44 potentially active volcanoes considered, de Silva and Francis, 1991). However, it is two orders of magnitude

higher when comparing it per unit of length of arc (*ca.* 5x10-4 $km^3 y^{-1} km^{-1}$ for Parinacota volcano and 3.1x10-6 $km^3 y^{-1} km^{-1}$ for Central Andes active volcanoes, Francis and Hawkesworth, 1994). Considering all Parinacota volcano eruptive history, the difference is smaller (one order of magnitude, *ca.* 3.2x10-5 $km^3 y^{-1} km^{-1}$ for Parinacota volcano since Late Pleistocene), but still puts it as one of the most active volcanoes in the Central Andes in the Late Quaternary.

## VOLCANIC HAZARDS

Parinacota volcano is probably one of the most active volcanoes in the Central Andes of Northern Chile in Holocene times, which suggests that it is very likely to erupt in the next decades or centuries. Although located in a very remote area, its activity can affect small villages located to the east in Bolivia (Sajama) and the main international road connecting Chile and Bolivia (which is located in the southern shore of Chungará Lake). On the other hand, this area is a Chilean National Park and a World Biosphere Reserve with a very rich variety of altiplanic flora and fauna, whose habitat might be strongly affected in case of a new eruption.

Parinacota volcano Holocene activity can be divided into two main types, with different associated volcanic hazards. These types correspond to those eruptions formed through the central vent and those formed through flank parasite centres. The central vent activity is the most important in recent times and has mainly consisted of the generation of lava flows, pyroclastic flows and their associated tephra fallout deposits, and lahars. Pyroclastic flows have been directed in almost all directions from the main vent in recent times. Nowadays, the occurrence of one of these flows could affect directly or indirectly people living in the area, depending on its direction. If the flow is directed towards the south it can reach the Chungará Lake and might reach its southern shore affecting the main Chilean Custom Buildings of the Chile-Bolivia International road. If the flow is directed towards the northeast or east it can affect the extensive 'bofedal' (water meadows) areas, which are used by local people to keep and feed their animals (mainly llamas and alpacas), therefore, affecting local people's economy. If the flow is finally directed towards the west it can reach the Cotacotani lakes area, which is part of the Lauca National Park, affecting the flora and fauna living in the area.

The occurrence of a pyroclastic flow will be accompanied by tephra fallout, which will be mainly directed towards the east according to the main wind direction, affecting the Río Sajama bofedales, which are used to keep and feed thousands of domestic animals. The generation of lava flows through the main cone does not pose any direct threat, but the presence of a permanent ice cap on top of the volcano means that lahars are very likely to be formed as has been the case in other ice capped volcanoes in Soth America in very recent times, like Nevado del Ruiz volcano, Colombia in 1985 and Villarrica volcano in Chile in 1964, 1971 and 1984 (H. Moreno)[1]. Their extension will depend both on the volume of the ice-cap and snow accumulated and the eruption rate. An eruption between November and March is very likely to generate larger lahars, as it is the period of maximum precipitation in the area. Holocene lahars have not reached any area today populated, and the major environmental hazard associated to these flows could occur if they reach the northern shore of Chungará Lake, affecting the lake's flora and fauna habitat.

Less important for the environment have been the flank eruptions, the last of which probably occurred *ca.* 1,600 years ago (Wörner *et al.*, 2000a). All the flank eruptions of Parinacota volcano have occurred through two main fractures, which means they are very likely to be used again in case of a new flank eruption, especially the northern one (NNE trend), which has concentrated the latest activity. These eruptions have only produced lava flows of limited extent and the formation of small pyroclastic cones, not representing major threats to the flora and fauna of the surrounding areas. The major hazard could be related if a long lasting eruption occurs, which can generate tephra fallout deposits that could reach the bofedal areas, especially in Bolivia, and, therefore, affecting the domestic animal food supply for a long period of time.

## PALAEOGEOGRAPHIC CONSIDERATIONS

Recently, several studies have been carried out in the Altiplano of Chile and Bolivia to better

[1] 1993. Geología y Peligros del volcán Villarrica, regiones IX y X, Andes del Sur. Informe Proyecto Fondecyt 1247 (Unpublished), *Servicio Nacional de Geología y Minería*, 112 p.

understand the climatic evolution of the area in recent times, especially during the Late Pleistocene to Holocene. Most of these studies are based on sedimentological and isotopic approaches (Schwalb *et al.*, 1999; Sylvestre *et al.*, 1999; Argollo and Mourguiat, 2000; Ammann *et al.*, 2001). The authors' aim in this section is to contribute, based on their mainly field volcanology approach, to a better understanding of some palaeogeographic constraints related to the climatic evolution of this part of the Altiplano in Late Quaternary times.

As proposed by Clavero *et al.* (2002), Parinacota volcano was built on top of an active lacustrine basin located in the north-eastern part of the Lauca basin (Kött *et al.*, 1995; Gaupp *et al.*, 1999; Figs. 2, 3). Most of this area of the Chilean high Andes was glaciated in the Late Pleistocene according to the extensive moraine fields found in the area (Amman *et al.*, 2001). These extensive moraine fields probably dammed the Lauca river in the western part of the area, near Chucuyo (Fig. 3) in the Late Pleistocene, after the glaciers started to retreat and formed a large lake basin, which was probably separated from the southern Lauca basin (García *et al.*, 2004). The age of these extensive moraine fields has been suggested to be older than *ca.* 12,000 years by Amman *et al.* (2001), based on a $C^{14}$ date obtained from bottom sediments of the Cotacotani lakes area. Based on the authors' new data and that presented by Clavero *et al.* (2002), it is suggested that the minimum age from the NII stage moraines of Amman *et al.* (2001) is 8 ka BP, and therefore, could be younger, supporting their interpretation that NII glaciers in Northern Chile were not synchronous with the worldwide LGM (21 ka BP).

This lake basin developed with changes in lake-level, saline, moisture and evaporation conditions (Schwalb *et al.*, 1999). However, these authors correlated the latest evolution stages of this basin outcropping in the Cotacotani lakes area as being synchronous with the last evolution stages (Mid to Late Holocene) of nearby Lake Titicaca in Bolivia, based on the idea that sedimentation occurred in these basins after the emplacement of the debris avalanche, as argued by Clavero *et al.* (2002). The $C^{14}$ data presented by Clavero *et al.* (2002) do not support their Mid to Late Holocene age interpretation as the youngest date obtained in these sediments (on top of the sequence) yielded 10,650±80 BP, which is consistent with the fact that this basin was partly buried by the Parinacota debris avalanche *ca.* 8,000 years ago. This lake basin sedimentation could have been active in the area up to *ca.* 8,000 years BP, close in time to the Parinacota debris avalanche event, as suggested by the new date presented here from a peat layer in a kettle hole structure buried by an Ajata lava flow (Table 4). It is suggested that the palaeoclimatic evolution history of the upper Lauca lake basin proposed by Schwalb *et al.* (1999), should be reinterpreted and correlated to the Late Pleistocene-Early Holocene evolution history of Lake Titicaca and not to its Mid to Late Holocene history as it has been done.

## CONCLUSIONS

Parinacota volcano, located in the Central Andes Volcanic Zone, has been active since Late Pleistocene (*ca.* 300 ka). During the Holocene it has erupted more than 18 $km^3$ of magma, making it one of the most active volcanoes of the Central Andes of northern Chile in recent times.

It has evolved from a voluminous lava-dome complex in its earliest stage (Parinacota 1 unit, 300-70? ka), probably built during two main eruptive phases at around 260-300 ka and at 110-70 ka. The lava-dome complex was formed by rhyodacitic to rhyolitic domes, their associated block-and-ash flow deposits mainly directed to the west, dacitic coulées and andesitic lavas. In the Late Pleistocene-Holocene (Parinacota 2 unit, 70?-8 ka), it evolved to a steep-sided stratovolcano, mainly formed by silica-rich andesitic lava flows and minor tephra fallout deposits. Around 8 ka BP, the ancestral stratocone partially collapsed to the west, generating the Parinacota Debris Avalanche. The deposit extends for more than 23 km, covers an area of more than 140 $km^2$ and has an estimated minimum volume of 6 $km^3$. The authors propose that internal and external conditions of the ancestral Parinacota volcano and its substratum were very favourable to its collapse *ca.* 8,000 years ago.

The loading of the edifice on top of a ductile substratum would have caused its deformation, leading to the edifice to spread. Some east-west extension might have occurred associated to NNE and NS regional and local fissures due to dyke intrusions, and finally the intrusion of a viscous cryptodome probably deformed enough the edifice to trigger its collapse. Soon after the partial collapse of the ancestral volcano a new stratocone started to build (Parinacota 3, <8 ka), formed by andesitic lava flows, andesitic to dacitic pyroclastic flow and tephra fallout deposits, and lahar deposits. Simultaneously, a series of flanks cones (6-1.4 ka) was formed in the south-western flank of the volcano.

Parinacota 3 explosive activity has produced numerous sub-plinian eruptions, which have generated pyroclastic flows, directed in all directions around the volcano. Parinacota volcano last eruption produced a pyroclastic flow directed to the southern flank in historical times (<200 years BP). This explosive activity is probably the major environmental threat today to the surroundings of Parinacota volcano in case of renewal eruptive activity.

## ACKNOWLEDGEMENTS

This research was funded through a collaborative project between Sernageomin-Chile and Bristol University-UK. JEC acknowledges the support from Presidente de la República scolarship (Mideplan-Chile) and RSJS a NERC Professorship. $^{40}Ar/^{39}Ar$ dates were obtained through a NERC grant (RSJS and MSP) and $C^{14}$ dates through a collaborative project between Sernageomin and GSC-Canada. The authors gratefully acknowledge the help in the field provided by A. Díaz, S. Mánquez, M. Robles (Servicio Nacional de Geología y Minería, Chile), M. Gardeweg (Aurum Consultores, Chile), and especially to H. Uribe (Sergeomin-Bolivia) for his friendship and invaluable help during a short field trip to the Bolivian side of the Nevados de Payachata volcanic area. C. Espejo, F. Llona (Sernageomin, Chile) and J. Imlach (SURRC, UK) provided technical assistance to obtain geochemical and geochronological data. B.M. Brannstrom (GSC-Canada) kindly helped the authors to obtain more rapidly the $C^{14}$ data. Comments by S. Self (Open University, UK), and J. Blundy (University of Bristol, UK) on an early version are acknowledged. G. Wörner (Universität Göttingen, Germany) and J.A. Naranjo (Sernageomin, Chile) are gratefully acknowledged for their thorough, critical and very helpful reviews that improved the manuscript.

## REFERENCES

Aguirre, E. 1990. Geología del Complejo Volcánico Choquelimpie-Ajoya, Altiplano de Arica, I Región. Memoria de Título (Unpublished), *Universidad de Chile, Departamento de Geología,* 150 p.

Allmendinger, R.; Jordan, T.; Kay, S.; Isacks, B. 1997. The evolution of the Altiplano-Puna Plateau of the Central Andes. *Annual Review of Earth Planetary Science*, Vol. 25, p. 139-174.

Amman, C.; Jenny, B.; Kammer, K.; Messerli, B.; 2001. Late Quaternary Glacier response to humidity changes in the arid Andes of Chile (18-29°S). *Palaeogeography, Palaeoclimatology, Palaeoecology*, Vol. 172, p. 313-326.

Argollo, J.; Mourguiart, P. 2000. Late Quaternary climate history of the Bolivian Altiplano. *Quaternary International*, Vol. 72, p. 37-51.

Borgia, A. 1994. Dynamic basis of volcanic spreading. *Journal of Geophysical Research*, Vol. 99 (B9), p. 17791-17804.

Bourdon, B.; Wörner, G.; Zindler, A. 2000. U-series evidence for crustal involvement and magma residence times in the petrogenesis of Parinacota volcano, Chile. *Contributions to Mineralogy and Petrology*, Vol. 139, p. 458-469.

Cas, R.; Wright, R. 1987. Volcanic successions: Modern and Ancient. *Unwin and Hyman*, 540 p. London.

Clavero, J.E. 2002. Evolution of Parinacota volcano and Taapaca Volcanic Complex, Central Andes of Northern Chile. Ph.D. Thesis (Unpublished), *University of Bristol*, 212 p.

Clavero, J.E.; Moreno, H. 1994. Ignimbritas Licán y Pucón: evidencias de erupciones explosivas

andesítico-basálticas postglaciales del volcán Villarrica, Andes del Sur, 39°25'S. *In Congreso Geológico Chileno, No. 7, Actas,* Vol. 1, p. 250-254. Concepción.

Clavero, J.E. 1996. Ignimbritas andesítico-basálticas postglaciales del volcán Villarrica, Andes del Sur (39°25'S). Master Thesis (Unpublished), *Universidad de Chile, Departamento de Geología*, 112 p.

Clavero, J.; Sparks, R.S.J.; Huppert, H.; Dade, B. 2002. Geological constraints on the emplacement mechanism of the Parinacota debris avalanche, Northern Chile. *Bulletin of Volcanology,* Vol. 64, p. 40-54.

Crisp, J. 1984. Rates of magma emplacement and volcanic output. *Journal of Volcanology and Geothermal Research*, Vol. 20, p. 177-211.

de Silva, S.; Francis, P. 1991. Volcanoes of the Central Andes. *Springer-Verlag*, 216 p. Berlin.

Dalrymple, G.B.; Duffield W.A. 1988. High-Precision Ar-$^{40}$/Ar-$^{39}$ dating of Oligocene Rhyolites from the Mogollon-datil Volcanic Field Using a Continous Laser System. *Geophysical Research Letters*, Vol. 15, No. 5, p. 463-466.

Davidson, J.; McMillan, N.; Moorbath, S.; Wörner, G.; Harmon, R.; López, L. 1990. The Nevados de Payachata volcanic region (18°S/69°W, N. Chile) II. Evidence for widespread crustal involvement in Andean magmatism. *Contributions to Mineralogy and Petrology*, Vol. 105, p. 412-432.

Day, S.; Carracedo, J.; Guillou, H. 1997. Age and geometry of an aborted rift flank collapse: the San Andrés fault system, El Hierro, Canary Islands. *Geological Magazine*, Vol. 134, No. 4, p. 523-537.

Druitt, T.H.; Edwards, L.; Mellors, R.M.; Pyle, D.M.; Sparks, R.S.J.; Lanphere, M.; Davies, M.; Barriero, B. 1999. Santorini Volcano. *Geological Society of London, Memoir* No. 19, 165 p. London.

Elsworth, D.; Voight, B. 1995. Dike intrusion as a trigger for large earthquakes and the failure of volcano flanks. *Journal of Geophysical Research*, Vol. 100 (B4), p. 6005-6024.

Elsworth, D.; Day, S. 1999. Flank collapse triggered by intrusion: the Canarian and Cape Verde Archipelagoes. *Journal of Volcanology and Geothermal Research*, Vol. 94, p. 323-340.

Entenmann, J. 1994. Magmatic evolution of the Nevados de Payachata complex and the petrogenesis of basaltic andesites in the Central Volcanic Zone of Northern Chile. Ph.D. Thesis (Unpublished), *Universität Mainz,* 115 p. Germany.

Francis, P.W.; Self, S. 1987. Collapsing volcanoes. *Scientific American*, Vol. 255, p. 90-97.

Francis, P.W.; Wells, G. 1988. Landsat thematic mapper observations of debris avalanche deposits in the Central Andes. *Bulletin of Volcanology*, Vol. 50, p. 258-278.

Francis, P.; Hawkesworth, C. 1994. Late Cenozoic rates of magmatic activity in the Central Andes and their relationships to continental crust formation and thickening. *Journal of the Geological Society*, Vol. 151, p. 845-854.

García, M.; Hérail, G.; Charrier, R. 1999. Age and structure of the Oxaya Anticline: a major feature of the Miocene Compressive structures of northernmost Chile. *International Symposium of Andean Geodynamics,* No. 4, p. 249-252. Göttingen, Germany.

García, M. 2001. Evolution oligo-néogène de l'arc et de l'avant-arc de l'Altiplano (Andes Centrales, Coude d'Arica,18-19°S).Tectonique, volcanisme, sédimentation, géomorphologie et bilan érosion-sédimentation. Thèse de doctorat (Unpublished), *Université Joseph Fourrier*, 200 p. Grenoble, France.

García, M.; Gardeweg, M.; Clavero, J.; Hérail, G. 2004. Mapa Geológico de la Hoja Arica. *Servicio Nacional de Geología y Minería*, Chile.

Gardeweg, M.; Sparks, R.S.J.; Matthews, S. 1998. Evolution of Lascar Volcano, Northern Chile. *Journal of the Geological Society*, Vol. 155, p. 89-104.

Gaupp, R.; Kött, A.; Wörner, G. 1999. Paleoclimatic implications of Mio-Pliocene sedimentation in the high-altitude intra-arc Lauca Basin of northern Chile. *Palaeogeography, Palaeoclimatology, Palaeoecology*, Vol. 151, p. 79-100.

González, O. 1995. Volcanes de Chile. *Instituto Geográfico Militar*, 541 p. Santiago, Chile.

Hildreth, W.; Moorbath, S. 1988. Crustal contributions to arc magmatism in the Andes of Central Chile. *Contributions to Mineralogy and Petrology*, Vol. 108, p. 247-252.

Hoblitt, H.; Miller, C.; Vallance, J. 1981. Origin and stratigraphy of the deposit produced by the May 18 directed blast. In The 1980 eruptions of Mount St. Helens, Washington. *US Geological Survey,* Professional Paper 1250, p. 401-420.

Hürliman, M.; García-Piera, J.; Ledesma, A. 2000. Causes and mobility of large volcanic landslides: application to Tenerife, Canary Islands. *Journal of Volcanology and Geothermal Research*, Vol. 103, p. 121-134.

Jordan, E. 1999. Glaciers of Bolivia. *In* Satellite Atlas of Glaciers of the World. *US Geological Survey,* Professional Paper 1386-I, 206 p.

Katsui, Y.; González, O. 1968. Geología del área neovolcánica de los Nevados de Payachata. *Universidad de Chile, Departamento de Geología,* Publicación No. 29, 61 p.

Kött, A.; Gaupp, R.; Wörner, G. 1995. Miocene to Recent history of the western Altiplano in northern Chile revealed by lacustrine sediments of the Lauca Basin (18°15'-18°40'S/69°30'-69°05'W). *Geologische Rundschau*, Vol. 84, p. 770-780.

Le Maitre, R.W.; Baterman P.; Dudek A.; Keller J.; Lameyre Le Bas, M.J.; Sabine P.A.;H Schmid R.; Sorensen H.; Streckeisen A.; Woolley A.R.; Zanettin, B. 1989. A classification of igneous rocks and glossary of terms. *Blackwell*, 193 p. Oxford.

Lipman, P.; Moore, J.; Swanson, D. 1981. Bulging of the north flank before the May 18 eruption-geodetic data.

*In* The 1980 eruptions of Mount St. Helens, Washington. *US Geological Survey,* Professional Paper 1250, p. 143-156.

Lipman, P.; Lockwood, J.; Okamura, R.; Swanson, D.; Yamashita, K. 1985. Ground deformation associated with the 1975 magnitude-7.2 earthquake and resulting changes in activity of Kilauea volcano, Hawaii. *US Geological Survey*, Professional Paper 1276, 45 p.

McMillan, N.; Davidson, J.; Wörner, G.; Harmon, R.; Moorbath, S.; López, L. 1993. Influence of crustal thickening on arc magmatism: Nevados de Payachata volcanic region, northern Chile. *Geology*, Vol. 21, p. 467-470.

Maniken, E.A.; Dalrymple, G.B. 1972. The electron microprobe and K-Ar dating. *Earth and Planetary Science Letters*, Vol. 17, p. 89-94.

Merle, O.; Borgia, A. 1996. Scaled experiments of volcanic spreading. *Journal of Geophysical Research,* Vol. 101, p. 13805-13817.

Montecinos, F. 1963. Observaciones de Geología en el Cuadrángulo de Campanani, Departamento de Arica, Provincia de Tarapacá. Memoria de Título (Unpublished), *Universidad de Chile, Departamento de Geología,* 109 p.

Moore, J.; Clague, D.; Holcomb, R.; Lipman, P.; Normark, W.; Torresan, M. 1989. Prodigius submarine landslides on the Hawaiian Ridge. *Journal of Geophysical Research*, Vol. 94 (B12), p. 17465-17484.

Moreno, H.; Clavero, J.; Lara, L. 1994. Actividad explosiva postglacial del volcán Villarrica, Andes del Sur (39°25'S). *In Congreso Geológico Chileno, No. 7, Actas,* Vol. 1, p. 329-333. Concepción.

Muñoz, N.; Sepúlveda, P. 1992. Estructuras compresivas con vergencia al Oeste en el borde oriental de la Depresión Central, Norte de Chile (19°15'lat. S). *Revista Geológica de Chile*, Vol. 19. No. 2, p. 241-247.

Muñoz, N.; Charrier, R. 1996. Uplift of the western border of the Altiplano on a west-vergent thrust system, Northern Chile. *Journal of South American Earth Sciences*, Vol. 9, Nos. 3-4, p. 171-181.

Murphy, M.; Sparks, S.; Barclay, J.; Carroll, M.; Brewer, T. 2000. Remobilization of Andesite Magma by Intrusion of Mafic Magma at the Soufrière Hills Volcano, Montserrat, West Indies. *Journal of Petrology*, Vol. 41, No. 1, p. 21-42.

Naranjo, J.; Moreno, H. 1991. Actividad explosiva postglacial del volcán Llaima. *Revista Geológica de Chile*, Vol. 18, No. 1, p. 69-80.

Naranjo, J. 1992. Chemistry and petrological evolution of Lastarria volcanic complex in the north Chilean Andes. *Geological Magazine*, Vol. 129, p. 723-740.

Naranjo, J.; Moreno, H.; Banks, N. 1993. La erupción del volcán Hudson en 1991 (46°S), Región XI, Aisén, Chile. *Servicio Nacional de Geología y Minería, Chile, Boletín*, No. 44, 50 p.

Pacci, D.; Hervé, F.; Munizaga, F.; Kawashita K, Cordani, U. 1980. Acerca de la edad Rb/Sr precámbrica de rocas de la Formación Esquistos de Belén, Departamento de Parinacota, Chile. *Revista Geológica de Chile*, Vol. 11, p. 23-29.

Pallister, J.; Hoblitt, R.; Reyes, A. 1992. A basalt trigger for the 1991 eruptions of Pinatubo Volcano. *Nature,* Vol. 356, p. 426-428.

Petit-Breuilh, M.; Lobato, J. 1994. Análisis comparativo de la cronología eruptiva histórica de los volcanes Llaima y Villarrica (38°-39° L.S.). *In Congreso Geológico Chile, No. 7, Actas,* Vol. 1, p. 366-370. Concepción, Chile.

Petit-Breuilh, M. 1999. Cronología eruptiva histórica de los volcanes Osorno y Calbuco, Andes del Sur (41°-41°30'S). *Servicio Nacional de Geología y Minería, Boletín,* No. 53, 46 p.

Pinto, L.; G. Hérail, G.; Charrier, R. 2004. Sedimentación sintecónica asociada a las estructuras neógenas en la Precordillera de la zona de Moquella, Tarapacá (19°15'S), norte de Chile. *Revista Geológica de Chile*, Vol. 31, No. 1, p. 19-44.

Reiche, P. 1937. The Toreva block-A distinctive landslide type. *Journal of Geology*, Vol. 45, p. 538-548.

Scheuber, E.; Giese, P. 1999. Architecture of the Central Andes- a compilation of geoscientific data along a transect at 21°S. *Journal of South American Earth Sciences*, Vol. 12, p. 103-107.

Schwalb, A.; Burns, S.; Kelts, K. 1999. Holocene environments from stable isotope stratigraphy of ostracods and authigenic carbonate in Chilean Altiplano Lakes. *Palaeogeography, Palaeoclimatology, Palaeoecology,* Vol. 148, p. 153-168.

Siebert, L. 1984. Large volcanic debris avalanches: characteristics of source areas, deposits, and associated eruptions. *Journal of Volcanology and Geothermal Research*, Vol. 22, p. 163-197.

Simkin, T.; Siebert, L. 1994. Volcanoes of the World, 2nd edition. *Smithsonian Institution, Geoscience Press*, 349 p. Tucson.

Sparks, R.S.J.; Sigurdsson, H.; Wilson, L. 1977. Magma mixing: a mechanism for triggering acid explosive eruptions. *Nature*, Vol. 267, p. 315-318.

Steiger, R.H.; Jäger, E. 1977. Subcomission on geochronology: convention on the use of decay constants in geo-and cosmochronology. *Earth and Planetary Science Letters*, Vol. 36, p. 359-362.

Stern, C.R. 2004. Active Andean volcanism: its geologic and tectonic setting. *Revista Geológica de Chile*, Vol. 31, No. 2, p. 161-206.

Sylvestre, F.; Servant, M.; Servant-Vildary, S.; Causse, C.; Fournier, M.; Ybert, J. 1999. Lake-Level Chronology on the Southern Bolivian Altiplano (18°-23°S) during Late-Glacial Time and the Early Holocene. *Quaternary Research*, Vol. 51, p. 54-66.

Taylor, J.R. 1982. An introduction to error analysis. *University Science Books*, 270 p. Mill Valley, California.

Ui, T. 1983. Volcanic dry avalanche deposits: identifications and comparison with nonvolcanic debris stream deposits. *Journal of Volcanology and Geothermal Research*, Vol. 18, p. 135-150.

Van Wyk de Vries, B.; Borgia, A. 1996. The role of basement in volcano deformation. *In* Volcano instability on the earth and other Planets (Mcguire, W.J.; Jones, A.P.; Neuberg, J.; editors). *Geological Society of London,* Special Publication 110, p. 95-110.

Van Wyk de Vries, B.; Francis, P. 1997. Catastrophic collapse at stratovolcanoes induced by gradual volcano spreading. *Nature*, Vol. 387, p. 387-390.

Van Wyk de Vries, B.; Matela, R. 1998. Styles of volcano-induced deformation: numerical models of substratum flexure, spreading and extrusion. *Journal of Volcanology and Geothermal Research*, Vol. 81, p. 1-18.

Van Wyk de Vries, B.; Self, S.; Francis, P.; Keszthelyi, L. 2001. A gravitational spreading origin for the Socompa debris avalanche. *Journal of Volcanology and Geothermal Research*, Vol. 105, p. 225-247.

Wijbrans, J.R.; Pringle, M.S.; Kopper, A.A.P.; Scheveers, R. 1995. Argon geochronology of small samples using the Vulkaan argon laserprobe. *Proceedings of the Koninklijke Nederlandse Akademie van Wetenschappen,* Vol. 98, No. 2, p. 185-218.

Voight, B.; Glicken, H.; Janda, R.; Douglass, P. 1981. Catastrophic rockslide avalanche of May 18. *In* The 1980 eruptions of Mount St. Helens, Washington. *US Geological Survey*, Professional Paper 1250, p. 347-378.

Voight, B.; Elsworth, E. 1997. Failure of volcano slopes. *Géotechnique*, Vol. 47, No. 1, p. 1-31.

Wörner, G.; Harmon, R.; Davidson, J.; Moorbath, S.; Turner, D.; McMillan, N.; Nye, C.; López, L.; Moreno, H. 1988. The Nevados de Payachata volcanic region (18°S/69°W, N. Chile) I. Geological, geochemical and isotopic observations. *Bulletin of Volcanology*, Vol. 50, p. 287-303.

Wörner, G.; López, L.; Moorbath, S.; Horn, S.; Entenmann, J.; Harmon, R.; Davidson, J. 1992a. Variaciones geoquímicas, locales y regionales, en el frente volcánico cuaternario de los Andes Centrales (17°30'-22°00'S), Norte de Chile. *Revista Geológica de Chile*, Vol. 19, No. 1, p. 37-56.

Wörner, G.; Moorbath, S.; Harmon, R. 1992b. Andean Cenozoic volcanic centers reflect basement isotopic domains. *Geology*, Vol. 20, p. 1103-1106.

Wörner, G.; Hammerschmidt, K.; Henjes-Kunst, F.; Lzaun, J.; Wilke, H. 2000a. Geochronology ($^{40}Ar/^{39}Ar$, K-Ar and He-exposure ages) of Cenozoic magmatic rocks from northern Chile (18-22°S): implications for magmatism and tectonic evolution of the central Andes. *Revista Geológica de Chile*, Vol. 27, No. 2, p. 205-240.

Wörner, G.; Lezaun, J.; Beck, A.; Heber, V.; Lucassen, F.; Zinngrebe, E.; Rössling, R.; Wilke, H. 2000b. Precambrian and Early Paleozoic evolution of the Andean basement at Belen (northern Chile) and Cerro Uyarani (western Bolivia Altiplano). *Journal of South American Earth Sciences*, Vol. 13, p. 717-737.

York, D. 1969. Least squares fitting of a straight line with correlated errors. *Earth and Planetary Science Letters,* Vol. 5, p. 320-324.

Manuscript received: December 12, 2001; accepted: October, 14, 2004.